

TIGHT CONTACT STRUCTURES ON A FAMILY OF HYPERBOLIC L-SPACES

HYUNKI MIN AND ISACCO NONINO

ABSTRACT. We classify tight contact structures on various surgeries on the Whitehead link, which provides the first classification result on an infinite family of hyperbolic L-spaces. We also determine which of the tight contact structures are Stein fillable and which are virtually overtwisted.

1. INTRODUCTION

A cooriented contact 3-manifold (M, ξ) is *overtwisted* if it contains an overtwisted disk, which is an embedded disk tangent to the contact planes along the boundary, and *tight* if it does not contain an overtwisted disk. Since Eliashberg [11] classified overtwisted contact structures, more recent studies focus on the classification of tight contact structures.

Since tight contact structures respect the prime decomposition of 3-manifolds by the work of Colin [3] (see also [9, 33]), it is sufficient to consider the classification of tight contact structures on prime manifolds. The geometrization of 3-manifolds implies that a prime 3-manifold is either Seifert fibered, toroidal or hyperbolic. For Seifert fibered spaces with two singular fibers, tight contact structures were completely classified, see [12, 15, 26, 31]. For Seifert fibered spaces with three singular fibers, there have been several classification results, see [20, 24, 23, 54, 55] for example. For toroidal case, tight contact structures were classified on torus bundles over S^1 and S^1 -bundles over a surface, see [25, 26, 27, 32, 37]. Honda, Kazez and Matic [34] showed that there exist infinitely many tight contact structures up to isotopy on toroidal manifolds and Colin, Giroux and Honda [5] showed that a closed orientable irreducible 3-manifold supports infinitely many tight contact structures up to isotopy if and only if it is toroidal.

For hyperbolic manifolds, much less is known although most 3-manifolds fall into this category [52]. Honda, Kazez and Matic [35] partially classified tight contact structures on hyperbolic surface bundles over S^1 when the contact structures have an *extremal* relative Euler class, meaning that the Euler class of the contact structure evaluated on a fiber surface is maximal. Later, Conway and the first author [7] classified tight contact structures on (most) surgeries on the figure eight knot in S^3 , which contain infinitely many hyperbolic 3-manifolds.

In this paper we will consider hyperbolic L-spaces. Recall that an *L-space* is a rational homology sphere such that the order of the first singular homology group equals the free rank of its Heegaard Floer homology group. In general, it is hard to construct a universally tight contact structure on an L-space because an L-space does not admit a

taut foliation, which can be perturbed into a universally tight contact structure. There are some non-hyperbolic L-spaces (e.g. lens spaces) that support a universally tight contact structure while it is not known for hyperbolic L-spaces yet. Thus it is natural to ask whether there is a hyperbolic L-space that supports a universally tight contact structure, which can be considered as a contact topology version of the L-space conjecture.

Conjecture 1.1. *A hyperbolic 3-manifold is an L-space if and only if it does not support a universally tight contact structure.*

Notice that none of the hyperbolic manifolds mentioned above are an L-space, and they all admit a taut foliation so support universally tight contact structures. In this paper, we classify tight contact structures on an infinite family of hyperbolic L-spaces and show that most of them are virtually overtwisted.

Let $M(n, r)$ be the result of (n, r) -surgery on the Whitehead link, see Figure 1. We will classify tight contact structures on $M(n, r)$ for surgery coefficients

$$\begin{aligned} n &\in \mathbb{Z}, n \geq 5, \\ r &\in \mathcal{R}_+ \cup \mathbb{Q}_-, \end{aligned}$$

where \mathbb{Q}_- is the set of negative rational numbers and

$$\mathcal{R}_+ = ([2, 4) \cup [5, \infty)) \cap \mathbb{Q}.$$

Recall that the Whitehead link is a hyperbolic L-space link. In particular, Liu [43, Proposition 6.4] showed that $M(r_1, r_2)$ is an L-space if and only if $r_1, r_2 > 0$. Moreover, there are only finitely many (26) isolated exceptional Dehn fillings of the Whitehead link [45, 53]. Thus our family of $M(n, r)$ contains infinite many hyperbolic L-spaces.

Before stating the results, we define two functions $\Phi(r)$ and $\Psi(r)$. For $0 < r \leq 1$, we write the negative continued fraction of $-\frac{1}{r}$ as follows:

$$-\frac{1}{r} = [r_0, \dots, r_n] = r_0 - \frac{1}{r_1 - \frac{1}{\dots - \frac{1}{r_n}}},$$

where $r_0 \leq -1$, and $r_i \leq -2$ for $i = 1, \dots, n$. Then define

$$\Phi(r) = |r_0(r_1 + 1) \cdots (r_n + 1)|.$$

We define Φ on all of \mathbb{Q} by setting $\Phi(r + 1) = \Phi(r)$. Then we define $\Psi(r)$ for $r \in \mathbb{Q}$ by

$$\Psi(r) = \begin{cases} 0 & r = 1 \\ \Phi(\frac{1}{1-r}) & r \neq 1 \end{cases}.$$

Now we are ready to state the main theorem of the paper.

Theorem 1.2. *Let $n \geq 5$ be an integer. Then $M(n, r)$ supports*

$$\begin{cases} \Psi(r) + 2\Phi(r) & r \in \mathcal{R}_+ \\ \Psi(r) & r \in \mathbb{Q}_- \end{cases}$$

tight contact structures up to isotopy, distinguished by their contact invariants in Heegaard Floer homology.

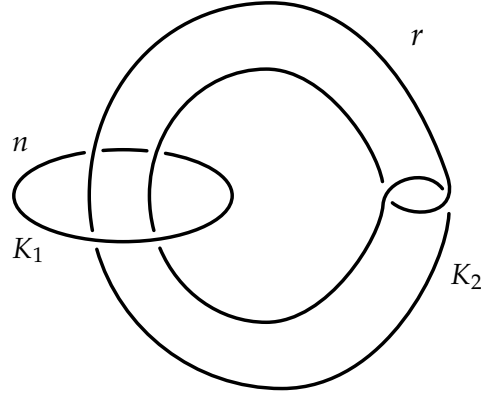


FIGURE 1. (n, r) -surgery on the Whitehead link.

Remark 1.3. For $n > 2$ and $r \geq 1$ (resp. $r < 1$), we can construct at least $\Psi(r) + 2\Phi(r)$ (resp. $\Psi(r)$) tight contact structures on $M(n, r)$ even if $n < 5$ or $r \notin \mathcal{R}_+$ (resp. $r \notin \mathcal{Q}_-$), see Section 3. However, there could be more.

We will prove Theorem 1.2 by estimating an upper bound using convex surface decompositions, and realizing this upper bound via contact surgery. We construct tight contact structures in Section 3 by using contact surgery diagrams and distinguish them by using the contact invariant in Heegaard Floer homology. In Section 4, we use a convex decomposition for a punctured genus one surface bundle over S^1 with a pseudo-Anosov monodromy, which was first introduced by Etnyre and Honda [19] and developed by Conway and the first author [7] for the figure-eight knot complement. In this paper, we generalize this technique for any pseudo-Anosov monodromy ϕ with $-1 < c(\phi) < 1$ where $c(\phi)$ is the fractional Dehn twist coefficient of ϕ . We expect this technique will apply to various monodromies and lead to the classification of tight contact structures on a broad class of hyperbolic 3-manifolds.

Recall that $M(n, 0)$ is a torus bundle over S^1 (see Section 4.1). Since $\Phi(m) = 1$ and $\Psi(m) = 2$ for any integer $m > 2$ and $\Psi(m) = |m - 1|$ for any integer $m < 0$, we have the following results for integer surgeries.

Corollary 1.4. *Let $n \geq 5$ and $m \neq 1, 4$ be integers. Then $M(n, m)$ supports*

$$\begin{cases} |m - 1| & m < 0, \\ \infty & m = 0, \\ 3 & m = 2, \\ 4 & m > 2, m \neq 4 \end{cases}$$

tight contact structures up to isotopy.

Recall that $M(5, \frac{5}{2})$ is the Weeks manifold, known to have the smallest volume among closed hyperbolic 3-manifolds [21]. Since $\Phi(\frac{5}{2}) = 2$ and $\Psi(\frac{5}{2}) = 3$, we obtain the following result.

Corollary 1.5. *The Weeks manifold supports seven tight contact structures up to isotopy.*

In addition to classifying tight contact structures, we also determine whether these tight contact structures are Stein fillable.

Theorem 1.6. *Let $n \geq 5$ be an integer and $r \in \mathcal{R}_+ \cup \mathcal{Q}_-$. Then every tight contact structure on $M(n, r)$ is Stein fillable.*

Lastly, we consider Conjecture 1.1 for $M(n, r)$. We provide a lower bound on the number of tight contact structures on $M(n, r)$ that are virtually overtwisted.

Theorem 1.7. *Let $n \geq 5$ be an integer and $r \in \mathcal{R}_+ \cup \mathcal{Q}_-$. Then $M(n, r)$ supports at least*

$$\begin{cases} \Psi(r) + 2\Phi(r) - 6 & r \in \mathcal{R}_+ \\ \Psi(r) - 2 & r \in \mathcal{Q}_- \end{cases}$$

virtually overtwisted contact structures up to isotopy.

Remark 1.8. There are some cases (e.g. $r \geq 2$ integers) in which $\Psi(r) + 2\Phi(r)$ is smaller than 6. In these cases, it is uncertain whether any tight contact structure on $M(n, r)$ is universally tight or virtually overtwisted.

Acknowledgments. The authors thank James Conway and John Etnyre for their helpful comments on the first draft, Andy Wand and Ana Lecuona for their useful advices and Kenneth Baker for interesting comments on genus one fibered knots in lens spaces and their monodromies. The authors are also grateful to Lisa Piccirillo for a helpful discussion on surgery operations.

2. CONTACT TOPOLOGY PRELIMINARIES

We assume that the reader is familiar with basic 3-dimensional contact topology [16], including Legendrian knots [17], contact surgery, open book decomposition [18], convex surface theory [14, 31], and Heegaard Floer homology [48, 49]. In this section, we briefly review the results that we will frequently use.

2.1. Convex surfaces. Let (M, ξ) be a contact 3-manifold. Recall that a *contact vector field* is a vector field of which the flow preserves ξ . An orientable surface Σ is called *convex* if there exists a contact vector field transverse to Σ . If Σ has boundary, then we assume that $\partial \Sigma$ is Legendrian with negative twisting number with respect to the surface framing. According to *Giroux's flexibility theorem*, any embedded surface can be C^∞ -perturbed (rel boundary) into a convex surface.

Given a convex surface Σ , the *dividing set* Γ_Σ is a set of points on Σ where the contact vector field X is tangent to ξ . It can be shown that Γ_Σ is an embedded multicurve on Σ . The dividing set divides Σ into two regions:

$$\Sigma \setminus \Gamma_\Sigma = R_+ \cup R_-$$

where $R_+ = \{p \in \Sigma : \alpha(X_p) > 0\}$ and $R_- = \{p \in \Sigma : \alpha(X_p) < 0\}$. If Σ has Legendrian boundary, then $\text{tb}(\partial \Sigma) = -\frac{1}{2}|\Gamma_\Sigma \cap \partial \Sigma|$ and $\text{rot}(\partial \Sigma) = \chi(R_+) - \chi(R_-)$.

We denote the twisting number of a Legendrian curve γ with respect to a framing F by $\text{tw}(\gamma, F)$. We can easily compute the twisting number of a closed Legendrian curve on a convex surface.

Theorem 2.1 (Honda [31]). *Let γ be an embedded Legendrian closed curve on a convex surface Σ with a dividing set Γ_Σ . Then,*

$$\text{tw}(\gamma, \Sigma) = -\frac{|\gamma \cap \Gamma_\Sigma|}{2}$$

Let Σ be a convex surface with a dividing set Γ_Σ . We call a properly embedded graph G in Σ *non-isolating* if G intersect Γ_Σ transversely and every component of $\Sigma \setminus G$ intersects Γ_Σ .

Theorem 2.2 (Legendrian realization principle, Honda [31]). *If G is a properly embedded non-isolating graph on a convex surface Σ , then there is an isotopic copy of Σ relative to its boundary such that G is Legendrian.*

In particular, if $\Sigma \setminus G$ is connected, G can always be realized as a Legendrian graph. This implies any non-separating curve on Σ can be realized as a Legendrian curve.

Honda [31] showed that if two convex surfaces intersect along a Legendrian curve L , the dividing curves interleave and we can obtain a new convex surface by *rounding the edge*, see Figure 2.

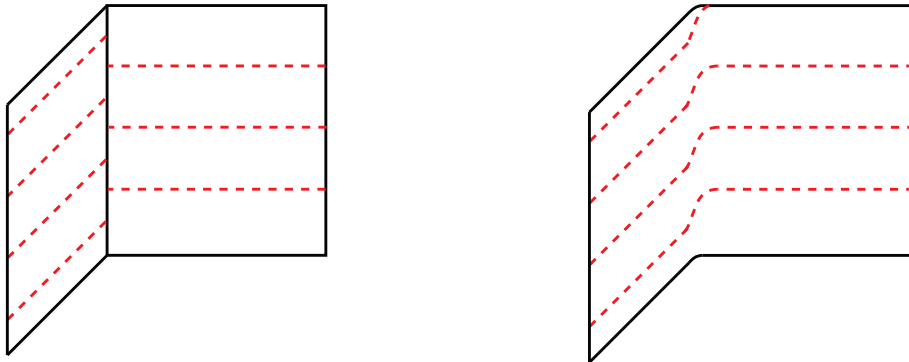


FIGURE 2. Rounding an edge between two convex surfaces.

We can modify a dividing set in a systematical way. Let Σ be an oriented convex surface with a dividing set Γ_Σ and D be a disk with Legendrian boundary with $\text{tb}(\partial D) = -1$. Suppose $\alpha = D \cap \Sigma$ intersects Γ_Σ in three points $\{p, q, r\}$ and $\partial\alpha = \{p, r\}$ are elliptic singularity of D . By Giroux's flexibility theorem, we can perturb D for q to be a unique hyperbolic singularity. We call D a *bypass* and the sign of the hyperbolic singularity is called the *sign* of a bypass.

Honda proved in [31] that there is a one-sided neighborhood $\Sigma \times [0, 1]$ of $\Sigma \cup D$ such that $\Sigma \times \{0, 1\}$ is convex and the dividing set on $\Sigma \times \{1\}$ is modified as shown in Figure 3. We say $\Sigma \times \{1\}$ is obtained from $\Sigma \times \{0\}$ by a bypass attachment along α . Note that a bypass can be on either side of a surface and it gives a different effect on the dividing set.

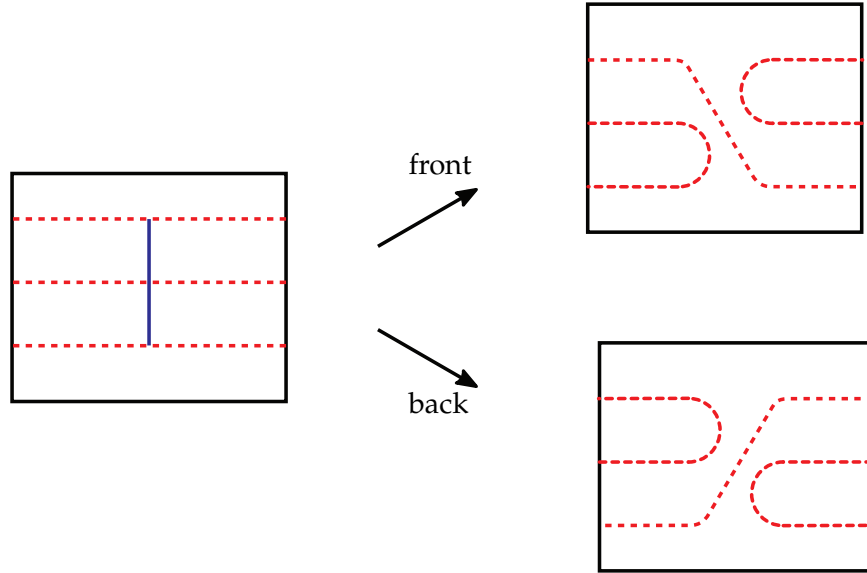


FIGURE 3. Bypass attachments

Let us investigate the effect of bypass attachment to a torus in detail. First, we introduce the Farey graph. We define the graph inductively. Let \mathbb{D} be the Poincaré disk. Start with the top-most vertex labeled $0 = \frac{0}{1}$ and the bottom-most vertex labeled $\infty = \frac{1}{0}$ and connect them by a geodesic. Given two vertices in the right half plane which are already labeled $\frac{a}{b}$ and $\frac{c}{d}$, choose a vertex on $\partial\mathbb{D}$ in the middle of the vertices and label it as $\frac{a+c}{b+d}$. Then connect it with the other two vertices by geodesics. For the left half plane, we treat ∞ as $-\infty = \frac{-1}{0}$. See Figure 4.

Now consider a convex torus T^2 with two parallel dividing curves and a linear characteristic foliation. We call a leaf of this characteristic foliation a *ruling curve*. Choose a homology basis for T^2 as $(\binom{1}{0}, \binom{0}{1})$. Denote the slope of curves parallel to $\binom{p}{q}$ by $\frac{p}{q}$.

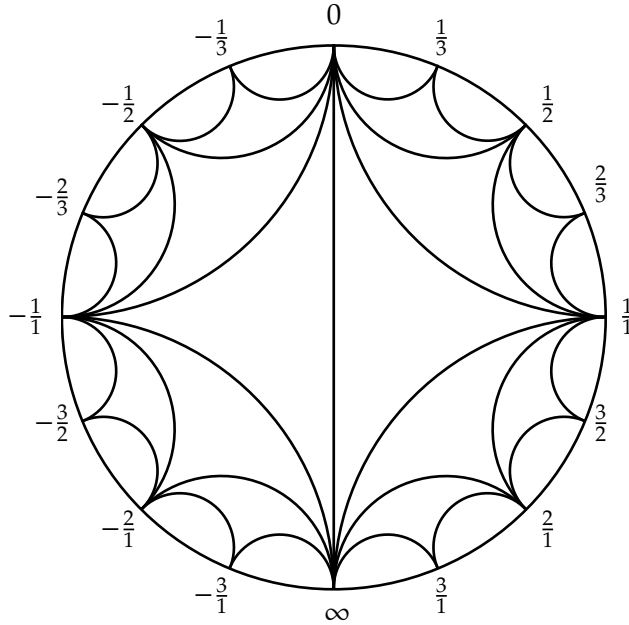


FIGURE 4. The Farey graph

Theorem 2.3 (Honda [31]). *Let s, r be the dividing slope and the ruling slope of T^2 respectively. After a bypass attachment along a ruling curve, we obtain a new convex torus with two dividing curves with slope s' , where s' is the vertex on the Farey graph anticlockwise of r and clockwise of s . In addition, s' is closest to r with an edge to s .*

Remark 2.4. In Theorem 2.3, we use the slope convention $\frac{p}{q} = \begin{pmatrix} p \\ q \end{pmatrix}$ since $\frac{\text{meridian}}{\text{longitude}}$ is our slope convention for a solid torus. If we use the slope convention $\frac{q}{p} = \begin{pmatrix} p \\ q \end{pmatrix}$, then we should reverse the words “clockwise” and “anticlockwise”. Also, Theorem 2.3 assumes that we attach a bypass from the front. If we attach a bypass from the back, then we should reverse the words “clockwise” and “anticlockwise”.

We need to guarantee the existence of bypasses to utilize them. There are several ways to find bypasses.

Theorem 2.5 (Imbalance principle, Honda [31]). *Let Σ and $A = S^1 \times [0, 1]$ be convex surfaces with Legendrian boundary. Suppose $\Sigma \cap A = S^1 \times \{0\}$ and $\text{tw}(S^1 \times \{0\}) < \text{tw}(S^1 \times \{1\}) \leq 0$. Then there is a bypass for Σ along $S^1 \times \{0\}$.*

Theorem 2.6 (Disk imbalance, Honda [31]). *Let Σ be a convex surface and D be a convex disk with a Legendrian boundary. Suppose $\Sigma \cap D = \partial D$. If $\text{tb}(\partial D) < -1$ then there is a bypass for Σ along ∂D .*

Theorem 2.7 (Bypass rotation, Honda–Kazez–Matić [36]). *Suppose that there is a bypass for Σ from the front along an attaching arc γ . If γ' is a Legendrian arc as in Figure 5, then there exists a bypass for Σ from the front along γ' .*

Theorem 2.8 (Bypass slide, Honda [31]). *Suppose that there is a bypass for Σ from the front along an attaching arc γ . If γ' is a Legendrian arc that is isotopic to γ relative to Γ_Σ , then there is a bypass for Σ from the front along γ' .*

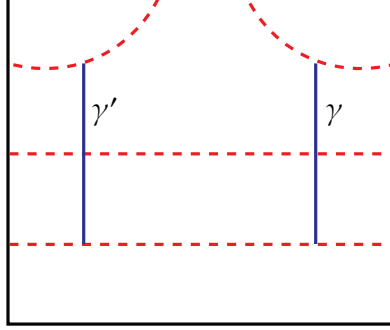


FIGURE 5. The attaching arc for a bypass rotation.

2.2. Contact structures on $T^2 \times I$ and solid tori. A tight contact structure ξ on $T^2 \times I$ is called a *basic slice* if

- (1) $\partial(T^2 \times I) = T_0 \cup T_1$ is two standard convex tori with dividing slopes s_0 and s_1 , respectively,
- (2) s_0 and s_1 are connected by an edge in the Farey graph, and
- (3) the slope of the dividing curves on any convex torus T parallel to the boundary is clockwise of s_0 and anticlockwise of s_1 in the Farey graph. This condition is called *minimal twisting*.

Honda [31] studied various properties of basic slices. Here, we review the classification of basic slices up to isotopy.

Theorem 2.9 (Honda [31]). *There are exactly two basic slices up to isotopy fixing the characteristic foliation on the boundary. These two tight contact structures are distinguished by their relative Euler class. They are called positive and negative basic slices and denoted by $B_+(s_0, s_1)$ and $B_-(s_0, s_1)$, respectively.*

We now review Giroux torsion. Let $k \in \frac{1}{2}\mathbb{N}$. Consider the contact structure $\xi^k = \ker(\sin(2\pi kz)dx + \cos(2\pi kz)dy)$ on $T^2 \times [0, 1]$, where (x, y) are the coordinates on T^2 and z is the coordinate on $[0, 1]$. We call ξ^k a *Giroux k -torsion layer* and if we have a contact structure (M, ξ) into which $(T^2 \times [0, 1], \xi^k)$ embeds, we say (M, ξ) contains *Giroux k -torsion*. We will use the phrase (M, ξ) has *exactly Giroux k -torsion* to the situation where one can embed $(T^2 \times [0, 1], \xi^k)$ into (M, ξ) but not $(T^2 \times [0, 1], \xi^{k+\frac{1}{2}})$. If $k = 1/2$, then we

call ξ^k a *half Giroux torsion*. We say (M, ξ) has *no (half) Giroux torsion* if $(T^2 \times [0, 1], \xi^k)$ does not embed in (M, ξ) for any $k \in \frac{1}{2}\mathbb{N}$.

Now we consider $(T^2 \times \mathbb{R}, \sin(2\pi kz)dx + \cos(2\pi kz)dy)$ and perturb $T^2 \times \{0\}$ and $T^2 \times \{1\}$ so that they become convex with two dividing curves of slope 0. Let ξ_c^k be the resulting contact structure on $T^2 \times [0, 1]$. We call this ξ_c^k a *convex Giroux k -torsion layer*. Notice that inside of $(T^2 \times [0, 1], \xi_c^k)$ there is a basic slice with one boundary component agreeing with $T^2 \times \{0\}$ and having boundary slope 0 and ∞ . This will either be a positive or a negative basic slice. By reversing the coorientation of ξ_c^k , if necessary, we can assume it is positive.

Theorem 2.10. *For $k \in \frac{1}{2}\mathbb{N}$, there are exactly two convex Giroux k -torsions $\pm\xi_c^k$, up to isotopy, on $T^2 \times [0, 1]$ with convex boundary having two dividing curves, both of slope r . The two contact structures are contactomorphic.*

Remark 2.11. In this paper, since we only consider contact manifolds with convex boundary, we just use the term *Giroux k -torsion* for convex Giroux k -torsion. However, readers should notice that the original Giroux torsion has pre-Lagrangian torus boundary.

Next, we will review the classification of tight contact structures on a solid torus. Consider a solid torus with a fixed longitude. Here, our slope convention is $\frac{\text{meridian}}{\text{longitude}}$. We denote by $N(s)$, a solid torus with convex boundary having two dividing curves of slope s .

Theorem 2.12 (Giroux [26], Honda [31]). *Let (p, q) be a pair relatively prime integers satisfying $q > -p \geq 1$ and*

$$\frac{q}{p} = [r_0, \dots, r_k]$$

for $r_i \leq -2$. Then there exist

$$|(r_0 + 1) \dots (r_{k-1} + 1)r_k|$$

tight contact structures on $N(\frac{p}{q})$ up to isotopy fixing the characteristic foliation on the boundary.

Now we consider a solid torus with a different meridional slope. Take a core of $N(s)$ and perform an r -surgery on it. Then we obtain a solid torus with dividing slope s and meridional slope r . Denote it by $N_r(s)$. From Theorem 2.12, we can deduce the following result.

Proposition 2.13 (Conway–Min [7]). *Let (p, q) be a pair relatively prime integers. Then there exist $\Phi(\frac{p}{q})$ tight contact structures on $N_{p/q}(\infty)$ up to isotopy fixing the characteristic foliation on the boundary.*

2.3. Contact surgery. Let L be a Legendrian knot in a contact 3-manifold (M, ξ) and N a standard neighborhood of L . *Contact $(\frac{p}{q})$ -surgery* on L is defined as follows: let (μ, λ) be a meridian and contact framing of L , respectively. $(M_{(p/q)}(L), \xi_{(p/q)})$ is obtained by cutting N from M and re-gluing it via a diffeomorphism of ∂N sending μ to $p\mu + q\lambda$. Then, extend the contact structure $(M \setminus N, \xi)$ to the entire $M_{(p/q)}(L)$. In general, the extension

is not unique since there could be distinct tight contact structures on N with a given boundary condition. If we only focus on the tight contact structures on N , Theorem 2.12 provides the number of all possible extensions.

Theorem 2.14 (Ding and Geiges [8]). *Let L be a Legendrian knot in (M, ξ) and p, q be relatively prime integers satisfying $\frac{p}{q} < 0$. The number of contact structure induced by contact $(\frac{p}{q})$ -surgery on L is*

$$|(r_0 + 1) \cdots (r_n + 1)|$$

where

$$\frac{p}{q} = r_0 + 1 - \frac{1}{r_1 - \frac{1}{r_2 \cdots \frac{1}{r_n}}}$$

for $r_i \leq -2$.

If $\frac{p}{q} > 0$, use $\frac{p}{q-kp}$ instead where k is a positive integer such that $q - kp < 0$.

In [10], Ding, Geiges and Stipsicz exhibited an algorithm that converts any contact surgery diagram into a (± 1) -surgery diagram.

- contact $(\frac{p}{q})$ -surgery with $\frac{p}{q} < 0$:
 - (1) Stabilize L $|r_0 + 2|$ times. Let this be L_0 .
 - (2) For $i = 1, \dots, n$, let L_i be the Legendrian push-off of L_{i-1} and stabilize it $|r_i + 2|$ times.
 - (3) Then a contact $(\frac{p}{q})$ -surgery on L corresponds to a contact (-1) -surgeries on a link (L_0, \dots, L_n) .
- contact $(\frac{p}{q})$ -surgery with $\frac{p}{q} > 0$:
 - (1) Choose a positive integer k such that $q - kp < 0$. Let $r' = \frac{p}{q-kp}$.
 - (2) Let L_1, \dots, L_k be k successive Legendrian push-offs of L .
 - (3) Then a contact $(\frac{p}{q})$ -surgery on L corresponds to $(+1)$ -surgeries on L, L_1, \dots, L_{k-1} and a contact (r') -surgery on L_k .

Sometimes, a contact surgery produces an overtwisted contact structure.

Proposition 2.15. *A contact (r) -surgery on a Legendrian knot L results in an overtwisted contact structure if*

- $r = 0$ and L is any Legendrian knot,
- $0 < r < 1$ and L is a Legendrian unknot with $\text{tb} = -1$.

2.4. Contact invariants in Heegaard Floer homology. In this subsection, we review some useful properties of contact invariants in Heegaard Floer homology.

Theorem 2.16 (Ozsváth and Szabó [50], Ghiggini [22]). *The Heegaard Floer contact invariant $c(\xi) \in \widehat{\text{HF}}(-M)$ of (M, ξ) satisfies the following properties.*

- If (M, ξ) is overtwisted, then $c(\xi) = 0$.
- If (M, ξ) is strongly fillable, then $c(\xi) \neq 0$.

- Let L be a Legendrian knot in (M, ξ) and (M_L, ξ_L) the result of Legendrian surgery on L . If $c(\xi) \neq 0$, then $c(\xi_L) \neq 0$.

There also have been several studies when a positive contact surgery preserves non-vanishing contact invariants, see [28, 41, 42, 44]. In this paper, we only need the result for the right-handed trefoil.

Theorem 2.17 (Lisca and Stipsicz [41]). *Let L be a Legendrian right-handed trefoil in (S^3, ξ_{std}) with $tb(L) = 1$. For any $r \in \mathbb{Q} \setminus \{0\}$, contact (r) -surgery on L produces a tight contact structure with non-vanishing contact invariant.*

3. THE LOWER BOUNDS

In this section, we will construct $2\Phi(r) + \Psi(r)$ isotopy classes of tight contact structures on $M(n, r)$ for $n > 2$ and $r \geq 1$ and $\Psi(r)$ isotopy classes of tight contact structures for $n > 2$ and $r < 1$ using contact surgery diagrams. We first construct contact structures counted by Ψ and then consider contact structures counted by Φ . After that, we will show that the contact structures counted by Ψ are distinct from the ones counted by Φ .

3.1. Tight contact structures counted by Ψ . Consider the surgery diagram for $M(n, r)$ shown in Figure 1. A left-handed Rolfsen twist on K_1 turns the diagram into the one in Figure 6. We then perform a sequence of inverse slam-dunk moves to turn K_1 into a chain of unknots. Since we have

$$-\frac{n+1}{n} = \overbrace{[-2, \dots, -2]}^n,$$

there are n components in the chain of the unknots and the surgery coefficients are all -2 , see Figure 7. We can turn this diagram into a contact surgery diagram as shown in Figure 8. Applying the algorithm in Section 2.3, we can convert the diagram into a (± 1) -contact surgery diagram. Notice that there are choices of stabilizations during the conversion.

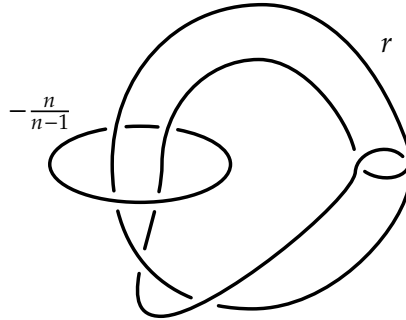


FIGURE 6. A surgery diagram for $M(n, r)$.

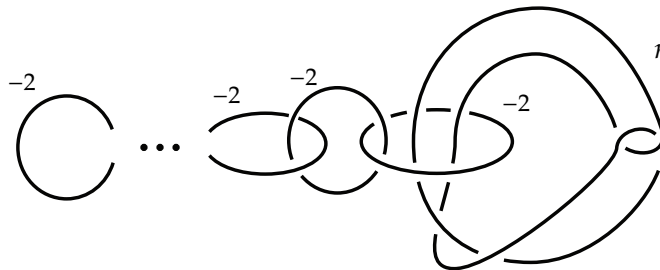
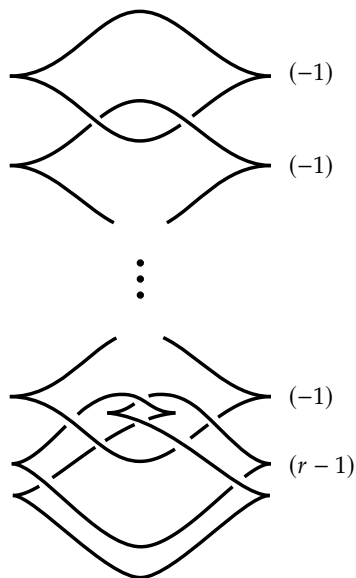


FIGURE 7. The result of inverse slam–dunk moves.

FIGURE 8. A contact surgery diagram for tight contact structures on $M(n, r)$ counted by Ψ .

Proposition 3.1. *The contact surgery diagram in Figure 8 induces a tight contact structure for any choice of stabilizations for any $r \neq 1$.*

Proof. We first consider the case $r > 1$. Fix a choice of stabilizations. Since $r > 1$, the contact surgery coefficient on the trefoil component in Figure 8 is positive. Thus there exists a single link component L having contact surgery coefficient $(+1)$ after the conversion, and all other components have the contact surgery coefficient (-1) . Let $(S_2^3(L), \xi_L)$ be the result of a contact $(+1)$ -surgery on L . L is a Legendrian right-handed trefoil with $\text{tb}(L) = 1$, hence the Heegaard Floer invariant of ξ_L is non-vanishing by Theorem 2.17. Since the contact structure on $M(n, r)$ is constructed from $(S_2^3(L), \xi_L)$ by Legendrian surgeries on the other link components, the Heegaard Floer invariant of the resulting contact structure is non-vanishing by Theorem 2.16. Thus the contact structure on $M(n, r)$ is tight.

Now we consider the case $r < 1$. Fix a choice of stabilizations. Since $r < 1$, the contact surgery coefficient on the trefoil component in Figure 8 is negative. Thus this contact surgery diagram represents a Stein fillable contact structure and hence it is tight. \square

Proposition 3.2. *The contact surgery diagram in Figure 8 induces $\Psi(r)$ pairwise non-isotopic tight contact structures for any $r \in \mathbb{Q}$, distinguished by their Heegaard Floer invariants.*

Proof. We first consider the case $r > 1$. We will use the same notations used in Proposition 3.1. As we discussed in the proof of Proposition 3.1, there exists a single link component L with the contact surgery coefficient (+1) after the conversion, and all other components have the contact surgery coefficient (-1). Thus there exists a Stein cobordism W from $S_2^3(L)$ to $M(n, r)$ induced from the contact surgery diagram. We claim that different choices of stabilizations give rise to non-isomorphic Stein structures and by [51, Theorem 2] the induced contact structures on $M(n, r)$ are also non-isotopic, distinguished by their Heegaard Floer invariants. To prove the claim, fix two different choices of stabilizations. Suppose L_1, \dots, L_m are the push-offs of L after the conversion. Since each L_i is rationally null-homologous in $S_2^3(L)$, we can calculate its rational rotation number in $(S_2^3(L), \xi_L)$. Recall that a stabilization behaves precisely the same way as in the null-homologous case, i.e. $\text{rot}_{\mathbb{Q}}(S_{\pm}(L)) = \text{rot}_{\mathbb{Q}}(L) \pm 1$ (cf. [1, Lemma 1.3]).

Since we chose different sets of stabilizations, there exists at least one index i such that the values of $\text{rot}_{\mathbb{Q}}(L_i)$ are different. Now we compare the first Chern class of the Stein structure J induced by the surgery diagrams. Using the formula from [39, Lemma 4.1], we obtain

$$\langle c_1(J), [\Sigma_i \cup 2 \cdot C_i] \rangle = 2 \cdot \text{rot}_{\mathbb{Q}}(L_i),$$

where Σ_i is a rational Seifert surface of L_i , C_i is the core of the Weinstein 2-handle attached along L_i . Thus, the two different values of $\text{rot}_{\mathbb{Q}}(L_i)$ lead to non-isomorphic Stein structures, proving the claim.

By Proposition 3.1, all contact structures are tight for any choices of stabilizations. Hence we are only left to show that there exist $\Psi(r)$ different choices of stabilizations for the contact surgery diagram in Figure 8. According to the algorithm in Section 2.3, if $r > 1$, a contact $(r - 1)$ -surgery on L is equivalent to a contact (+1)-surgery on L and $(-\frac{r-1}{r-2})$ -surgery on its push-off. Consider the negative continued fraction expansion $-\frac{r-1}{r-2} = [r_0, r_1, \dots, r_k]$. Then the number of stabilization choices for a contact $(-\frac{r-1}{r-2})$ -surgery is $|r_0(r_1 + 1) \cdots (r_k + 1)|$, which is $\Phi(\frac{r-2}{r-1}) = \Phi(\frac{1}{1-r}) = \Psi(r)$.

If $r = 1$, we have $\Psi(1) = 0$ and the contact surgery diagram produces an overtwisted contact structure by Proposition 2.15.

Lastly, we consider the case $r < 1$. As discussed in Proposition 3.1, since all contact surgery coefficients are negative, the surgery diagram represents a Stein manifold (X, J) and the first Chern class of the Stein structure will evaluate to $\text{rot}(L_i)$ on the set of generators of $H_2(X; \mathbb{Z})$ given by the cores of 2-handles and the Seifert surfaces for the attaching spheres, see [29]. Since we chose different sets of stabilizations, there exists at least one index i such that the values of $\text{rot}(L_i)$ are different. Thus, the two different values of

$\text{rot}(L_i)$ lead to non-isomorphic Stein structures. Now we remain to show that there exist $\Psi(r)$ different choices of stabilizations for the contact surgery diagram in Figure 8. Consider the negative continued fraction expansion $r - 1 = [r_0, r_1, \dots, r_k]$. According to the algorithm in Section 2.3, the number of stabilization choices for a contact $(r - 1)$ -surgery is $|r_0(r_1 + 1) \cdots (r_k + 1)|$, which is $\Phi(\frac{1}{1-r}) = \Psi(r)$. \square

3.2. Tight contact structures counted by Φ . Since the Whitehead link is symmetric, we can switch the link components as shown in the first drawing of Figure 9. Perform a left-handed Rolfsen twist on K_2 , and we obtain a surgery diagram as shown in the right drawing of Figure 9. After realizing this link as a Legendrian link, we obtain a contact surgery diagram shown in Figure 10. Applying the algorithm from Section 2.3, we can convert the diagram into a (± 1) -contact surgery diagram. Again, there are choices of stabilizations during the conversion.

The proofs of Proposition 3.3 and 3.5 are essentially identical to the proofs of Proposition 3.1 and 3.2, respectively. We leave the first one as an exercise for the readers.

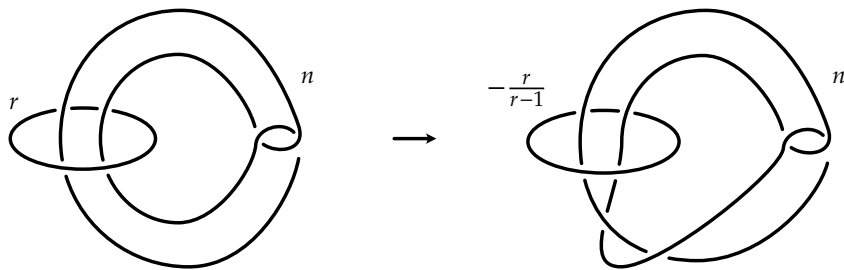


FIGURE 9. Another surgery diagram for $M(n, r)$.

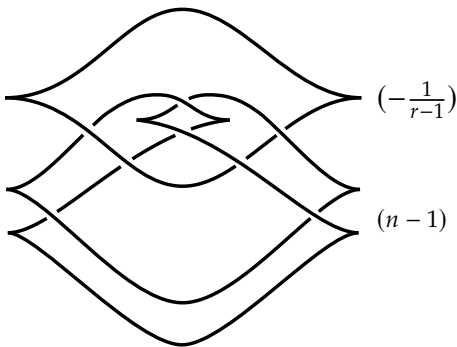


FIGURE 10. A contact surgery diagram for tight contact structures on $M(n, r)$ counted by Φ .

Proposition 3.3. *The contact surgery diagram in Figure 10 induces a tight contact structure for any choices of stabilizations for $r \geq 1$.* \square

Remark 3.4. By Proposition 2.15, the surgery diagram in Figure 10 results in overtwisted contact structures if $r < 0$.

Proposition 3.5. *The contact surgery diagram in Figure 10 induces $2\Phi(r)$ pairwise non-isotopic tight contact structures for $r \geq 1$, distinguished by their Heegaard Floer invariants.*

Proof. Similar to the proof of Proposition 3.1, there exists a single link component L with the contact surgery coefficient $(+1)$ after the conversion, and all other components have the contact surgery coefficient (-1) . Thus there exists a Stein cobordism W from $S^3_2(L)$ to $M(r)$ induced from the surgery diagram. As in the proof of Proposition 3.2, different choices of stabilizations give rise to non-isomorphic Stein structures on W and hence to non-isotopic contact structures on $M(n, r)$.

By Proposition 3.3, all contact structures are tight for any choices of stabilizations. Thus we are only left to show that there exist $2\Phi(r)$ different choices of stabilizations for the contact surgery diagram in Figure 10. According to the algorithm in Section 2.3, there exists two choices of stabilizations for a contact $(n - 1)$ -surgery. For a contact $(-\frac{1}{r-1})$ -surgery, consider the negative continued fraction expansion of $-\frac{1}{r-1} = [r_0, r_1, \dots, r_k]$. Then the number of stabilization choices for a contact $(-\frac{1}{r-1})$ -surgery is $|r_0(r_1 + 1) \cdots (r_k + 1)|$, which is $\Phi(r - 1) = \Phi(r)$. \square

3.3. Distinguishing contact structures counted by Ψ and Φ . So far, we have constructed tight contact structures on $M(n, r)$ using contact surgery diagrams. However, since we have used different surgery diagrams for the ones counted by Ψ and Φ , respectively, we constructed two distinct manifolds diffeomorphic to $M(n, r)$. To compare the isotopy classes of the contact structures on each manifold, we push them to a fixed manifold and determine their first Chern classes.

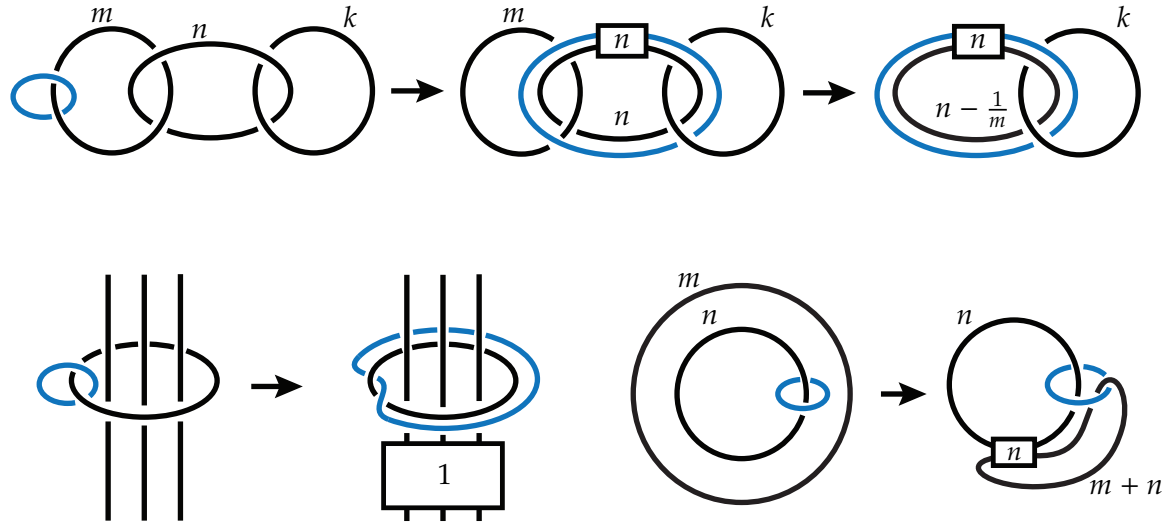


FIGURE 11. Various surgery operations.

Proposition 3.6. *For $n > 2$ and $r \geq 1$, $M(n, r)$ supports at least $\Psi(r) + 2\Phi(r)$ pairwise non-isotopic tight contact structures, distinguished by their Heegaard Floer invariants.*

Proof. In the previous subsections, we denoted by $M(n, r)$ any 3-manifolds constructed from the surgery diagrams in Figure 1, 7, 8, 9, and 10, but here we will distinguish them. Let $M(n, r)$ be the 3-manifold constructed from the surgery diagram shown in Figure 1, and M_1 a manifold constructed from the (± 1) -contact surgery diagram which is converted from Figure 8 using the algorithm in Section 2.3, and M_2 a manifold constructed from the (± 1) -contact surgery diagram converted from Figure 10. It is routine to check that we can return back from these (± 1) -contact surgery diagrams to the surgery diagram in Figure 1 by using isotopies (handle slides), slam-dunk moves and Rolfsen twists. Since each of these operations induces a diffeomorphism, we obtain diffeomorphisms $f^i: M_i \rightarrow M(n, r)$ for $i = 1, 2$.

Pick contact structures (M_1, ξ_1) and (M_2, ξ_2) counted by Ψ and Φ , respectively. We claim that the contact structures $f_*^1(\xi_1)$ and $f_*^2(\xi_2)$ on $M(n, r)$ are not isotopic. Together with Proposition 3.2 and 3.5, the claim completes the proof.

We will show the claim by calculating the first Chern classes of the contact structures. We start with calculating $H_1(M(n, r))$. Let μ and ν be the meridians of K_1 and K_2 in Figure 1, respectively. Since the linking number between the components of the Whitehead link is 0, we have

$$H_1(M(n, r)) = \langle \mu, \nu \mid n\mu = 0, p\nu = 0 \rangle = \mathbb{Z}_n \oplus \mathbb{Z}_p.$$

where $r = \frac{p}{q}$. Next, we will compute the Poincaré dual of $c_1(f_*^1(\xi_1))$ and express it in terms of $[\mu]$ and $[\nu]$. Consider the contact (± 1) -surgery diagram for (M_1, ξ_1) . Let $-\frac{r-1}{r-2} = [r_1, \dots, r_k]$, L_0 the Legendrian trefoil in Figure 8, and L_1, \dots, L_k its push-offs after the conversion. We also denote the Legendrian unknots in Figure 8 by $L'_1, L'_2, \dots, L'_{n-1}$ from the bottom to the top. According to the results from [10, 29], we have

$$(1) \quad \text{PD}(c_1(\xi_1)) = \sum_{i=0}^k \text{rot}(L_i)[\mu_i] + \sum_{i=1}^{n-1} \text{rot}(L'_i)[\mu'_i],$$

where $\text{rot}(L'_i) = 0$ for $1 \leq i \leq n-1$, $\text{rot}(L_0) = 0$ and $\text{rot}(L_i)$ for $1 \leq i \leq k$ depends on the choice of stabilizations. We now keep track of this homology class under the diffeomorphisms induced by surgery operations.

First, consider the chain of unknots L'_1, \dots, L'_{n-1} . We apply slam-dunk moves to remove all L'_i for $2 \leq i \leq n-1$. Suppose L'_i is the last component of the chain. We investigate the effect of a slam-dunk move to L'_i . We claim that the homology classes will change under the induced diffeomorphism as follows:

$$[\mu'_i] \mapsto -2[\mu'_{i-1}] - [\mu'_{i-2}]$$

and all other $[\mu_j]$ and $[\mu'_j]$ remained unchanged. To see this, slide μ'_i over L'_{i-1} and obtain a $(1, -2)$ -cable of L'_{i-1} as shown in the top of Figure 11. Thus we have $[\mu'_i] = -2[\mu'_{i-1}] +$

$[\lambda'_{i-1}]$ where λ'_{i-1} is a Seifert longitude of L'_{i-1} . Then apply the slam-dunk move to L'_i and remove it. Since the slam-dunk move is a local operation, it only affects a small neighborhood of $D'_i \cup L'_{i-1}$ where D'_i is a Seifert disk of L'_i . Thus it does not change the isotoped μ'_i . Also, λ'_{i-1} is isotopic to $-\mu'_{i-2}$ since $\text{lk}(L_i, L_{i-1}) = \text{tb}(L_{i-1}) = -1$. Thus the result follows.

Now we turn our attention to L_1, \dots, L_k . First, notice that the smooth surgery coefficient of L_0 is $2 = \text{tb}(L_0) + 1$, and all other L_i is $\text{tb}(L_i) - 1$. We slide L_k over L_{k-1} and L_k becomes a meridian of L_{k-1} . Since $\text{lk}(L_k, L_{k-1}) = \text{tb}(L_{k-1})$, the surgery coefficient becomes

$$\begin{aligned} (\text{tb}(L_k) - 1) + (\text{tb}(L_{k-1}) - 1) - 2 \text{tb}(L_{k-1}) &= \text{tb}(L_k) - \text{tb}(L_{k-1}) - 2 \\ &= r_k. \end{aligned}$$

The second equality follows from the fact that both $|r_k + 2|$ and $|\text{tb}(L_k) - \text{tb}(L_{k-1})|$ are the difference between the number of stabilizations on L_k and L_{k-1} . We keep sliding L_i over L_{i-1} for all $1 \leq i \leq k$ consecutively. Then we obtain a chain of unknots where $\text{lk}(L_i, L_{i-1}) = -1$ for $1 \leq i \leq k$. Notice that the surgery coefficient of L_i is

$$\begin{cases} \text{tb}(L_i) - \text{tb}(L_{i-1}) - 2 = r_i & 2 \leq i \leq k, \\ \text{tb}(L_i) - \text{tb}(L_{i-1}) = r_i + 1 & i = 1, \\ \text{tb}(L_i) + 1 = 2 & i = 0. \end{cases}$$

We can now perform a sequence of slam-dunk moves to eliminate all L_i for $1 \leq i \leq k$. Suppose L_i is the last component of the chain. As what we did to L'_i in the previous paragraph, we can keep track of the homology classes under the slam-dunk moves on L_i and the homology classes change as follows:

$$\begin{cases} [\mu_i] \mapsto r_{i-1}[\mu_{i-1}] - [\mu_{i-2}] & 3 \leq i \leq k \\ [\mu_i] \mapsto (r_{i-1} + 1)[\mu_{i-1}] - [\mu_{i-2}] & i = 2 \\ [\mu_i] \mapsto 2[\mu_{i-1}] & i = 1 \end{cases}$$

and all other $[\mu_j]$ and $[\mu'_j]$ remain unchanged.

Finally, we apply a right-handed Rolfsen twist along L'_1 and obtain the surgery diagram in Figure 1. As shown in the bottom left of Figure 11, the meridian μ'_1 becomes $(1, 1)$ -cable of L'_1 after the Rolfsen twist. Let λ'_1 be a Seifert longitude of L'_1 . Since the linking number between the two link components is 0, the homology classes will change under the induced diffeomorphism as follows:

$$[\mu'_1] \mapsto [\mu'_1] + [\lambda'_1] = [\mu'_1] + [\mu_0] - [\mu_0] = [\mu'_1],$$

and $[\mu_0]$ remains unchanged.

We can now naturally identify μ_0 and μ'_1 with ν and μ , respectively. Altogether, we have

$$\begin{aligned}
\text{PD}(c_1(f_*^1(\xi_1))) &= f_*^1(\text{PD}(c_1(\xi_1))) \\
&= f_*^1\left(\sum_{i=0}^k \text{rot}(L_i)[\mu_i] + \sum_{i=1}^{n-1} \text{rot}(L'_i)[\mu'_i]\right) \\
&= f_*^1\left(\sum_{i=0}^k \text{rot}(L_i)[\mu_i]\right) \\
&= \sum_{i=0}^k \text{rot}(L_i) \cdot f_*^1([\mu_i]) \\
&= 0[\mu] + m[\nu]
\end{aligned}$$

for some $m \in \mathbb{Z}$. The first and fourth equalities follow from the naturality, the second equality follows from (1), the third equality follows from the fact that $\text{rot}(L'_i) = 0$ for $1 \leq i \leq n-1$ and the fifth equality follows from the discussions about the effect of surgery operations in the previous paragraphs.

Similarly, we can calculate $c_1(f_*^2(\xi_2))$. Consider the contact (± 1) -surgery diagram for (M_2, ξ_2) . Let L_1 be the Legendrian trefoil in Figure 10. Since we have

$$\frac{n-1}{1-(n-1)} = -\frac{n-1}{n-2} = \overbrace{[-2, \dots, -2]}^{n-2},$$

there are $(n-2)$ push-offs of L_1 after the conversion. Denote them by L_2, L_3, \dots, L_{n-1} . Recall that during the conversion, we stabilize L_2 once and push it off $n-3$ times. Thus the rotation numbers of L_i are

$$(2) \quad \text{rot}(L_1) = 0, \text{rot}(L_2) = \text{rot}(L_3) = \dots = \text{rot}(L_{n-1}) = \pm 1.$$

Let L'_0, \dots, L'_k be the Legendrian unknot in Figure 10 and its push-offs after the conversion. As before, we have

$$(3) \quad \text{PD}(c_1(\xi_2)) = \sum_{i=1}^{n-1} \text{rot}(L_i)[\mu_i] + \sum_{i=0}^k \text{rot}(L'_i)[\mu'_i].$$

We first consider L_1, \dots, L_{n-1} . We start by sliding all L_i over L_1 for $2 \leq i \leq n-1$. This produces an unlink of $(n-2)$ components which are meridians of L_1 and the surgery coefficient of each component becomes -1 . The handle-slide operation on L_i induces a diffeomorphism and the homology classes will change under this diffeomorphism as follows:

$$[\mu_1] \mapsto [\mu_1] + [\mu_i]$$

and all other $[\mu_j]$ and $[\mu'_j]$ remain unchanged. This is clear from the bottom right of Figure 11. Now apply right-handed Rolfsen twist along each L_i for $2 \leq i \leq n-1$ and get

rid of it. As shown in the bottom left of Figure 11, each μ_i becomes a $(1, 1)$ -cable of L_i . Let λ_i be a Seifert longitude of L_i . Since λ_i is a meridian of L_1 and μ_i becomes contractible, the homology classes will change under the induced diffeomorphism as follows:

$$[\mu_i] \mapsto [\mu_i] + [\lambda_i] = [\mu_1]$$

and all other $[\mu_j]$ and $[\mu'_j]$ remain unchanged.

We now perform a sequence of handle-slides to make L'_0, \dots, L'_k a linear chain of unknots and then perform slam-dunk moves to get rid of all L'_i for $1 \leq i \leq k$. Thus we apply a similar argument as before to keep track of the homology classes. The only important fact here is that these operations only affect μ'_i and do not affect any μ_i .

Finally, we apply a right-handed Rolfsen twist along L'_0 and obtain the surgery diagram in the left of Figure 9. Then swap the link components and obtain the diagram in Figure 1. As in the case of ξ_1 , this Rolfsen twist does not affect any homology class.

We can now naturally identify μ_1 and μ'_0 with μ and ν , respectively. Altogether, we have

$$\begin{aligned} \text{PD}(c_1(f_*^2(\xi_2))) &= f_*^2(\text{PD}(c_1(\xi_2))) \\ &= f_*^2 \left(\sum_{i=1}^{n-1} \text{rot}(L_i)[\mu_i] + \sum_{i=0}^k \text{rot}(L'_i)[\mu'_i] \right) \\ &= \sum_{i=2}^{n-1} \pm f_*^2([\mu_i]) + \sum_{i=0}^k \text{rot}(L'_i) \cdot f_*^2([\mu'_i]) \\ &= \pm(n-2)[\mu] + h[\nu] \end{aligned}$$

for some $h \in \mathbb{Z}$. The first equality follows from the naturality, the second equality follows from (3), the third equality follows from (2) and the fourth equality follows from the discussions about the effect of surgery operations in the previous paragraphs.

Since we assume $n > 2$, we can conclude that $f_*^1(\xi_1)$ and $f_*^2(\xi_2)$ are distinguished by their first Chern classes, which completes the proof of the claim. \square

4. THE UPPER BOUNDS

In this section, we determine the upper bounds of the number tight contact structures on $M(n, r)$ for $n \geq 5$ and $r \in \mathcal{R}_+ \cup \mathbb{Q}_-$. Combining it with the lower bounds in Section 3, we complete the proof of Theorem 1.2.

4.1. Convex decompositions of $M(n, r)$. The first step is to decompose $M(n, r)$ into two pieces with convex torus boundary. Consider the surgery diagram for $M(n, r)$ shown in Figure 1. If we perform the surgery only on K_1 , then the result will be $L(n, n-1)$. Moreover, it is well known (c.f. [30, 47]) that K_2 is a genus one fibered knot in $L(n, n-1)$. Let N be a neighborhood of K_2 in $L(n, n-1)$, C_n the complement of N , Σ a fiber surface

of C_n and ϕ_n the monodromy of C_n . Then there is a symplectic basis of $H_1(\Sigma)$ such that the action of the monodromy ϕ_n on $H_1(\Sigma)$ is given by

$$\phi_n = \begin{pmatrix} -n+2 & 1 \\ -1 & 0 \end{pmatrix} = \begin{pmatrix} 1 & 0 \\ -1 & 1 \end{pmatrix} \begin{pmatrix} 1 & 1 \\ 0 & 1 \end{pmatrix} \begin{pmatrix} 1 & 0 \\ -1 & 1 \end{pmatrix}^{n-1}.$$

We can also assume that ϕ_n is the identity near the boundary. Notice that ϕ_n is pseudo-Anosov for $n \geq 5$, and the fractional Dehn twist coefficient $c(\phi_n) \in (0, 1)$ so ϕ_n is right-veering. Since $M(n, r)$ is a Dehn filling of C_n , we can write

$$M(n, r) = C_n \cup N_r$$

where N_r is a solid torus with the meridional slope r , with respect to the coordinate system induced by K_1 . We can also write C_n as

$$C_n = \Sigma \times [0, 1] / (x, 1) \sim (\phi_n(x), 0).$$

Let ξ be a contact structure on $M(n, r)$ and L a Legendrian knot in N_r isotopic to the core of N_r . We can assume that N_r is a standard neighborhood of L after a perturbation, so ∂N has convex boundary with two dividing curves of some slope s (again, we measure slopes on $\partial N_r = -\partial C_n$ using the coordinates induced by K_1). We will denote $C_n(s)$ and $N_r(s)$ when C_n and N_r have contact structures with convex boundaries with two dividing curves of slope s .

As was done in [7], we will *thicken* $C_n(s)$ into a standard form, which means finding $C_n(s') \subset C_n(s)$ such that $C_n(s) \setminus C_n(s') = T^2 \times I$. We say that $C_n(s)$ *thickens* to $C_n(s')$, or $C_n(s)$ *thickens to slope s'* . Also, we say $C_n(s)$ *does not thicken* if $C_n(s)$ thickens to s' implies $s = s'$. We will thicken $C(s)$ by attaching bypasses to $-\partial C_n(s)$. We will find such bypasses by finding boundary parallel dividing arcs on a fiber surface $\Sigma \subset C_n(s)$. Due to our slope convention and the choice of orientation, the slope increases after attaching a bypass to $-\partial C_n(s)$.

Let $\mathcal{S}(r)$ be the set of slopes s that is clockwise of r , anticlockwise of ∞ on the Farey graph and connected with r by an edge. For $r \in \mathcal{R}_+$, we need the following two lemmas.

Lemma 4.1. *Suppose $n \geq 5$, $r \in \mathcal{R}_+$ and $s \in \mathcal{S}(r)$. Then $C_n(s)$ thickens to $C_n(\infty)$.*

Once we thicken $C_n(s)$ to $C_n(\infty)$, we will determine an upper bound for the number of tight contact structures on $C_n(\infty)$.

Lemma 4.2. *Suppose there is no boundary parallel half Giroux torsion. Then there exist at most four tight contact structures on $C_n(\infty)$ up to isotopy (not fixing the boundary pointwise but preserving it setwise). Two of them thicken further to $C_n(1)$.*

Remark 4.3. Since we will classify tight contact structures on closed manifolds, which are obtained by gluing a solid torus to the boundary of $C_n(\infty)$, it is enough to classify tight contact structures on $C_n(\infty)$ up to isotopy fixing the boundary setwise.

For $r \in \mathcal{Q}_-$, we need the following two lemmas.

Lemma 4.4. *Suppose $n \geq 5$, $r \in \mathbb{Q}_-$, $s \in \mathcal{S}(r)$ and $s \neq 0$. Then $C_n(s)$ thickens to $C_n(1)$.*

According to Lemma 4.4, we can write $C_n(s) = T \cup C_n(1)$ for $s < 0$, where $T = T^2 \times [0, 1]$ with convex boundary and dividing slopes $s_0 = s$ and $s_1 = 1$.

Lemma 4.5. *Suppose there is no boundary parallel half Giroux torsion. Then there exist at most four tight contact structures on $C_n(-\frac{1}{k})$ for $k \in \mathbb{N}$ up to isotopy (not fixing the boundary pointwise but preserving it setwise). Moreover, the (possibly) tight contact structures on $C_n(-\frac{1}{k})$ are determined by their restriction to T .*

Remark 4.6. In fact, there are exactly three tight contact structures on $C_n(-1)$ without boundary parallel Giroux torsion but we will not use this fact in this paper.

We also need to count the number of tight contact structures on $N_r(\infty)$ and $N_r(1)$ using Proposition 2.13.

Lemma 4.7. *For any $r \in \mathbb{Q}$, there are $\Phi(r)$ tight contact structures on $N_r(\infty)$ up to isotopy fixing the boundary pointwise (hence fixing the characteristic foliation).*

Also, there are $\Psi(r)$ tight contact structures on $N_r(1)$ up to isotopy fixing the boundary pointwise.

Combining these lemmas, we can obtain the upper bounds.

Theorem 4.8. *Suppose $n \geq 5$ and $r \in \mathcal{R}_+ \cup \mathbb{Q}_-$.*

- $M(n, r)$ supports at most $2\Phi(r) + \Psi(r)$ tight contact structures up to isotopy if $r \in \mathcal{R}_+$.
- $M(n, r)$ supports at most $\Psi(r)$ tight contact structures up to isotopy if $r \in \mathbb{Q}_-$.

Proof. We first consider the case $r \in \mathcal{R}_+$. By Lemma 4.1 and Lemma 4.2, $C_n(s)$ thickens to slope ∞ or 1 for any $s \in \mathcal{S}(r)$. Thus any tight contact structure on $M(n, r)$ can be decomposed as a union of a tight contact structure on $C_n(\infty)$ and a tight contact structure on $N_r(\infty)$, or a union of a tight contact structure on $C_n(1)$ and a tight contact structure on $N_r(1)$. In the case that $C_n(s)$ thickens to $C_n(\infty)$ and not further, there are at most two tight contact structures on $C_n(\infty)$ by Lemma 4.2. Also, there are $\Phi(r)$ tight contact structure on $N_r(\infty)$ by Lemma 4.7. These lead to $2\Phi(r)$ (possibly) tight contact structures on $M(n, r)$. In the case that $C_n(s)$ thickens to $C_n(1)$, we can decompose $N_r(1)$ into a union of $N_r(-1)$ and T , where $T = T^2 \times I$ with dividing slopes -1 and 1 . By Lemma 4.5, a tight contact structure on $T \cup C_n(1) = C_n(-1)$ is completely determined by T . Also, there are $\Psi(r)$ tight contact structure on $N_r(-1) \cup T = N_r(1)$ by Lemma 4.7. These lead to the $\Psi(r)$ (possibly) tight contact structures on $M(n, r)$.

Next, we consider the case $r \in \mathbb{Q}_-$. By Lemma 4.4, $C_n(s)$ thickens to slope 1 for any $s \in \mathcal{S}(r)$ and $s \neq 0$. If $s = 0$, there is $N_r(s') \subset N_r(0)$ for $r < s' < 0$, so we can decompose $M(n, r)$ into $N_r(s')$ and $C_n(s')$. By Lemma 4.4, we can thicken $C_n(s')$ to slope 1. Thus any tight contact structure on $M(n, r)$ can be decomposed as a union of a tight contact structure on $C_n(1)$ and a tight contact structure on $N_r(1)$. We can decompose $N_r(1)$ into a union of $N_r(-\frac{1}{m})$ and T , where $m \in \mathbb{N}$ and $T = T^2 \times I$ with dividing slopes $-\frac{1}{m}$ and 1 .

By Lemma 4.5, a tight contact structure on $T \cup C_n(1) = C_n(-\frac{1}{m})$ is completely determined by T . Also, there are $\Psi(r)$ tight contact structure on $N_r(-\frac{1}{m}) \cup T = N_r(1)$ by Lemma 4.7. These lead to the $\Psi(r)$ (possibly) tight contact structures on $M(n, r)$. \square

We will prove the above lemmas in Section 4.4.

4.2. Normalizing the dividing set on Σ . We begin by normalizing the dividing set Γ_Σ of Σ . Since we can freely modify the slopes of the Legendrian ruling curves on N , we assume Σ is convex with Legendrian boundary.

Etnyre and Honda [19] normalized Γ_Σ for any pseudo-Anosov monodromy.

Proposition 4.9 (Etnyre and Honda [19]). *Suppose Γ_Σ consists of $k > 0$ properly embedded arcs and m closed curves. Then there is an isotopic copy of Σ such that one of the following holds.*

- (1) k is odd.
 - $m = 1$ and all arcs are in the same isotopy class that is not boundary parallel.
 - $m = 0$ and there are three distinct isotopy classes of arcs that are not boundary parallel.
 - there is a boundary parallel arc (possibly with other dividing curves).
- (2) k is even.
 - there is a boundary parallel arc (possibly with other dividing curves).

When $k \geq 3$, Etnyre and Honda [19] further normalized the dividing set on Σ in the figure-eight knot complement. Their argument holds however for any pseudo-Anosov monodromy.

Let ϕ be a pseudo-Anosov monodromy of $C = \Sigma \times [0, 1]/(x, 1) \sim (\phi(x), 0)$. Consider the matrix representation of ϕ with respect to the symplectic basis of Σ . Then there are two eigenvectors v_a and v_r , where v_a is an attracting fixed point of ϕ and v_r is a repelling fixed point of ϕ . Denote by s_a and s_r the slopes of v_a and v_r , respectively. There are two paths P_c and P_a in the Farey graph where P_c is the clockwise path from s_r to s_a and P_a is the anticlockwise path from s_r to s_a .

Lemma 4.10 (Etnyre and Honda [19]). *Suppose Γ_Σ consists of $k \geq 3$ properly embedded arcs and m closed curves. Then there is an isotopic copy of Σ such that one of the following holds.*

- $m = 0$ and there are three distinct isotopy classes of arcs with slopes $\{a, b, c\}$ in P_c . Moreover, $\{a, b, c\}$ forms the largest geodesic triangle in the Farey graph among geodesic triangles with vertices in P_c .
- $m = 0$ and there are three distinct isotopy classes of arcs with slopes $\{a, b, c\}$ in P_a . Moreover, $\{a, b, c\}$ forms the largest geodesic triangle in the Farey graph among geodesic triangles with vertices in P_a .
- there is a boundary parallel arc (possibly with other dividing curves).

Etnyre and Honda further convert these dividing sets into a simpler form.

Lemma 4.11 (Etnyre and Honda [19]). *Suppose that Γ_Σ consists of n arcs and there are three isotopy classes of arcs with slopes $\{a, b, c\}$ in P_a (resp. P_c). Without loss of generality, assume that a is the closest to s_r in the Farey graph. Then there is another isotopic copy of Σ such that*

- Γ_Σ consists of one closed curve and n arcs with slope a .
- there is a boundary parallel arc (possibly with other dividing curves).

Now we are ready to normalize the dividing set on Σ in our $C_n(s)$.

Proposition 4.12. *Suppose $\Sigma \subset C_n(s)$ and Γ_Σ consists of $k \geq 2$ properly embedded arcs and m closed curves. Then there is an isotopic copy of Σ such that one of the following holds.*

- (1) k is odd.
 - $m = 1$ and all dividing arcs have slope ∞ .
 - $m = 0$ and there are three isotopy classes of dividing arcs with slopes $\{0, 1, \infty\}$, $\text{mult}(1) = k - 2$ and $\text{mult}(0) = \text{mult}(\infty) = 1$. Here, $\text{mult}(s)$ is the number of arcs with slope s .
 - there is a boundary parallel arc (possibly with other dividing curves).
- (2) k is even, and there is a boundary parallel arc (possibly with other dividing curves).

Proof. Assume that any isotopic copy of Σ in $C_n(s)$ contains a boundary parallel dividing arc. By Proposition 4.9, this implies that k is odd. We first calculate the slopes of the fixed points v_a^n and v_r^n of ϕ_n for $n \geq 5$ and obtain

$$s_a^n = \frac{2}{n-2+\sqrt{n^2-4n}} \quad \text{and} \quad s_r^n = \frac{2}{n-2-\sqrt{n^2-4n}}.$$

Thus $0 < s_a^n < 1/2$ and $2 < s_r^n < \infty$. For any $n \geq 5$, the largest geodesic triangle with the vertices in P_c^n is $\{\infty, -1, 0\}$, and the largest geodesic triangle with the vertices in P_a^n is $\{\frac{1}{2}, \frac{2}{3}, 1\}$. By Lemma 4.10 and 4.11, there is an isotopic copy of Σ such that

- Γ_Σ consists of one closed curve and k arcs with slope ∞ , or
- Γ_Σ consists of one closed curve and k arcs with slope 1.

We claim that for the second case there is another isotopic copy of Σ such that there is a boundary parallel arc, or there are three isotopy classes of dividing arcs with slopes $\{0, 1, \infty\}$, $\text{mult}(1) = k - 2$ and $\text{mult}(0) = \text{mult}(\infty) = 1$. This claim will complete the proof.

We remain to prove the claim. Let U be a small I -invariant neighborhood of Σ in $C_n(s)$. Then $C_n(s) \setminus U = \Sigma \times [0, 1]$. Let $\Sigma_i := \Sigma \times \{i\}$ for $i = 0, 1$ and Γ_i be a dividing set of Σ_i . Then we have $\Gamma_1 = \Gamma_\Sigma$ and $\Gamma_0 = \phi_n(\Gamma_1)$.

We first consider the case $n > 5$. Take a closed curve c on Σ_1 with slope $\frac{1}{-n+3}$. Consider an annulus $c \times [0, 1]$ and let $c_i = c \times \{i\}$ for $i = 0, 1$. Assume c_i intersects Γ_i minimally. Then $|c_1 \cap \Gamma_1| = (n-2)(k+1)$ and $|c_0 \cap \Gamma_0| = 0$. Thus there is a bypass on A along c_1 . If the bypass does not straddle the closed dividing curve, attaching the bypass results in a boundary parallel arc (here, we attach the bypass from the back). If the bypass straddles the closed dividing curve, attaching the bypass results in the dividing set with slope $\{0, 1, \infty\}$ where $\text{mult}(1) = k - 2$ and $\text{mult}(0) = \text{mult}(\infty) = 1$.

Now if $n = 5$, take a closed curve c on Σ_1 with slope $\frac{2}{5}$. Consider an annulus $c \times [0, 1]$ and let $c_i = c \times \{i\}$ for $i = 0, 1$. Assume c_i intersects Γ_i minimally. Then $|c_1 \cap \Gamma_1| = 3(k+1)$ and $|c_0 \cap \Gamma_0| = k+1$. Thus there is a bypass on A along c_1 . If the bypass does not straddle the closed dividing curve, attaching the bypass results in a boundary parallel arc. If the bypass straddles the closed dividing curve, attaching the bypass results in the dividing set with slope $\{0, 1, \infty\}$ where $\text{mult}(1) = k-2$ and $\text{mult}(0) = \text{mult}(\infty) = 1$. \square

We also consider the case for $k = 1$ without boundary parallel half Giroux torsion.

Proposition 4.13. *Suppose there is no boundary parallel half Giroux torsion in $C_n(s)$ and Γ_Σ consists of one properly embedded arc and m closed curves. Then there exists an isotopic copy of Σ in $C_n(s)$ such that*

- one arc and one closed curve with slope ∞ .
- one boundary parallel arc without any other dividing curves.

We will prove this proposition in Section 4.4.

4.3. Thickening $C_n(s)$. Here, we will prove Lemma 4.1. We will thicken $C_n(s)$ to $C_n(s')$ by finding a bypass for $-\partial C_n(s)$ along $\partial \Sigma$. Recall that due to our slope conventions, this bypass has slope 0 on $\partial C_n(s)$ and s will change clockwise on the Farey graph.

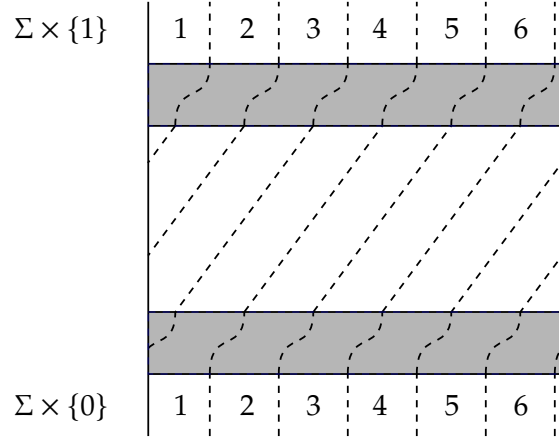


FIGURE 12. Edge rounding when $s = 3$. The left side is identified with the right side.

Proposition 4.14. *Suppose $s \geq 2$ and $s \notin \{\frac{4k+1}{k} \mid k \in \mathbb{N}\}$. Then there is an isotopic copy of Σ in $C_n(s)$ such that Γ_Σ contains a boundary parallel arc.*

Proof. Let $s = \frac{m}{k}$ for a pair of relatively prime positive integers m, k . There are m properly embedded dividing arcs on Σ . We cut $C_n(s)$ along Σ to obtain a genus-2 handlebody $\Sigma \times [0, 1]$ and round the edges to obtain a smooth convex boundary. Let Σ_i be $\Sigma \times \{i\}$ for $i = 0, 1$ and Γ_i the dividing set on Σ_i . Then $\Gamma_0 = \phi_n(\Gamma_1)$. After rounding the edges,

the entire dividing set only contains closed curves, but we will keep calling the dividing curves that pass through $\partial\Sigma$ dividing arcs for convenience.

For $i = 0, 1$, the dividing arcs in Γ_i divides $\partial\Sigma_i$ into $2m$ intervals, which we will label by 1 through $2m$. The dividing curves on $\partial\Sigma \times [0, 1]$ connect the i -th interval on Σ_1 to the $(i - 2k - 1)$ -th interval (mod $2m$) on Σ_0 . See Figure 12 for example.

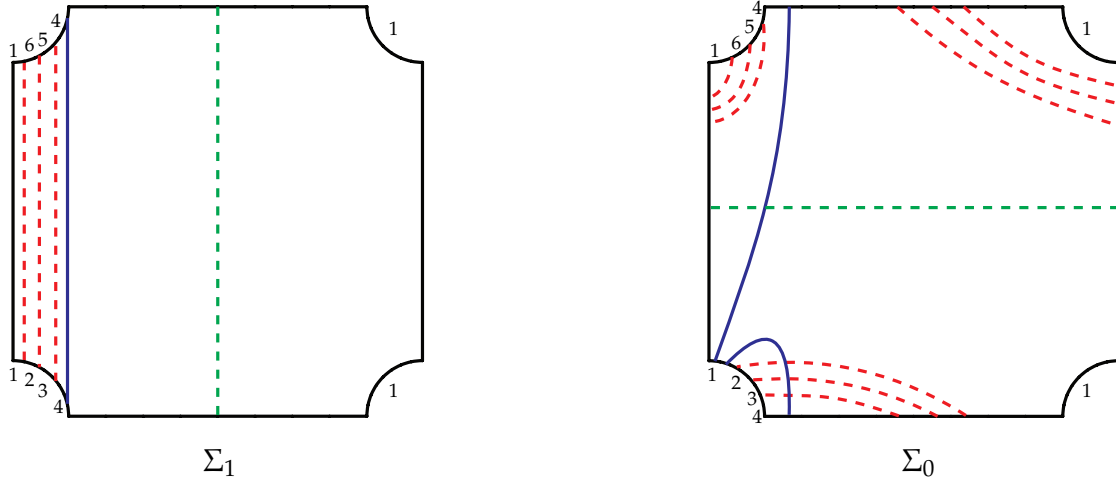


FIGURE 13. Σ_1 and Σ_0 in $C_n(3)$. The dotted lines are dividing curves. The blue lines are $\alpha \times \{1\}$ and $\alpha \times \{0\}$. In each drawing, the top and bottom sides are identified, and so are the left and right sides. In this figure, as well as in the rest of the paper, we draw Σ_0 with the orientation induced from the fibration $C_n(s)$, which disagrees with that induced by $\Sigma \times [0, 1]$. Also in this picture (and this picture only), we have enumerated the regions of $\partial\Sigma$ to better see the twisting of the dividing set as it runs over $\partial\Sigma \times [0, 1]$.

Suppose there is no boundary parallel dividing arc in Γ_i for $i = 0, 1$. By Proposition 4.12 and Proposition 4.13, we need to consider two cases.

(1) Γ_1 contains m arcs and one closed curve with slope ∞ : Let α be an arc on Σ_1 with slope ∞ that does not intersect Γ_1 . Let $D_\alpha := \alpha \times [0, 1]$ be a compressing disk for $\Sigma \times [0, 1]$. Perturb D_α so that its boundary does not intersect any dividing curve on $\partial\Sigma \times [0, 1]$. This results in a shift of the basepoints of α on Σ_0 by $(2k + 1)$ intervals following the negative orientation of $\partial\Sigma$, see Figure 13 for example. Thus ∂D_α only intersects the dividing curves on Σ_0 . We perturb D_α further so that it is convex with Legendrian boundary. We can also assume that ∂D_α intersects Γ_0 minimally, so it will intersect the closed dividing curve exactly once. Also, this intersection point separates $\alpha \times \{0\}$ into two sides. On one side it intersects $|2k + 1|$ dividing arcs, and on the other side it intersects $|m - (2k + 1)|$ dividing arcs. Since the total number of intersection points is greater than 2, there is a

bypass in D_α by Theorem 2.6. The difference between the number of intersections is:

$$d = ||m - 2k - 1| - |2k + 1|| = \begin{cases} |m - 4k - 2| & m \geq 2k + 1 \\ |m| & m < 2k + 1 \end{cases}$$

If $d \neq 1$, then the dividing curves on D_α cannot be nested as shown in the right drawing of Figure 14. Thus there is always a bypass which does not straddle the closed dividing curve. After attaching this bypass, we obtain an isotopic copy of Σ containing a boundary parallel dividing arc.

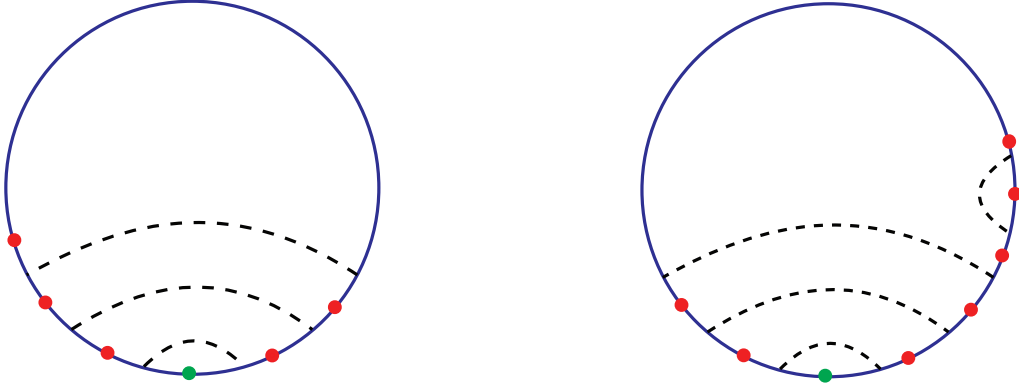


FIGURE 14. Dividing curves in D_α .

If $d = 1$, then $m = 1$, $m = 4k + 1$ or $m = 4k + 3$. Since we assume $s \geq 2$ and $s \neq \frac{4k+1}{k}$, we only need to consider the case $m = 4k + 3$. In this case, there are $2k + 2$ dividing curves on D_α and they can be nested as shown in the left drawing of Figure 14. Attach all $2k + 1$ bypasses to Σ_0 in sequence to obtain $\Sigma_{1/2}$ with dividing slopes $\{\infty, -1, 0\}$ such that $\text{mult}(\infty) = m - 2$ and $\text{mult}(-1) = \text{mult}(0) = 1$, see the right drawing of Figure 16. Then we can find an overtwisted disk as shown in Figure 16. Thus we can exclude this case too.

(2) $m \geq 3$ and Γ_1 contains arcs with slope $\{0, 1, \infty\}$ where $\text{mult}(0) = \text{mult}(\infty) = 1$ and $\text{mult}(1) = m - 2$: Let β be an arc on Σ_1 with slope ∞ that does not intersect Γ_1 , and $D_\beta := \beta \times [0, 1]$ be a compressing in $\Sigma \times [0, 1]$. We perturb D_β so that it is convex with Legendrian boundary, ∂D_β does not intersect the dividing curves on $\partial \Sigma \times [0, 1]$, and $\beta \times \{0\}$ intersects Γ_0 minimally, see Figure 17. Since $\beta \times \{0\}$ intersects more than four dividing curves in Γ_0 , we can find a bypass in D_β whose attaching arc lies on $\beta \times \{0\}$ by Theorem 2.6. From now on, we call dividing curves on Σ_0 with slopes $0, \frac{1}{n-2}$ and $\frac{1}{n-3}$ black, red and green dividing curves, respectively, see the right drawing of Figure 17. There are two cases we need to consider.

First, suppose $m > 3$. Since $s \geq 2$, we can assume that $m > 2k - 1$. In this case, the bypass cannot straddle the black dividing curve, see the right drawing of Figure 17.

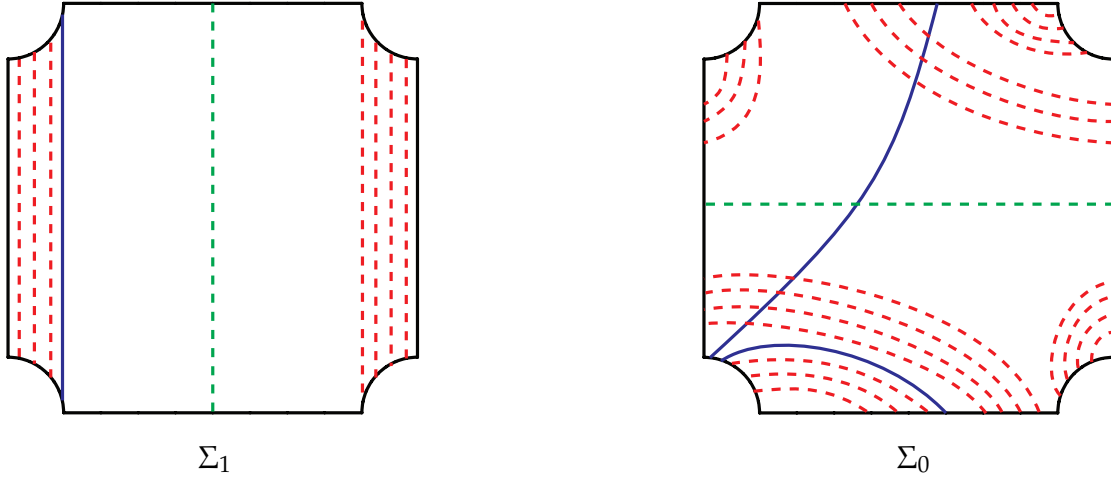


FIGURE 15. Σ_1 and Σ_0 in $C_n(7)$. The dotted lines are dividing curves and the blue lines are $\alpha \times \{1\}$ and $\alpha \times \{0\}$

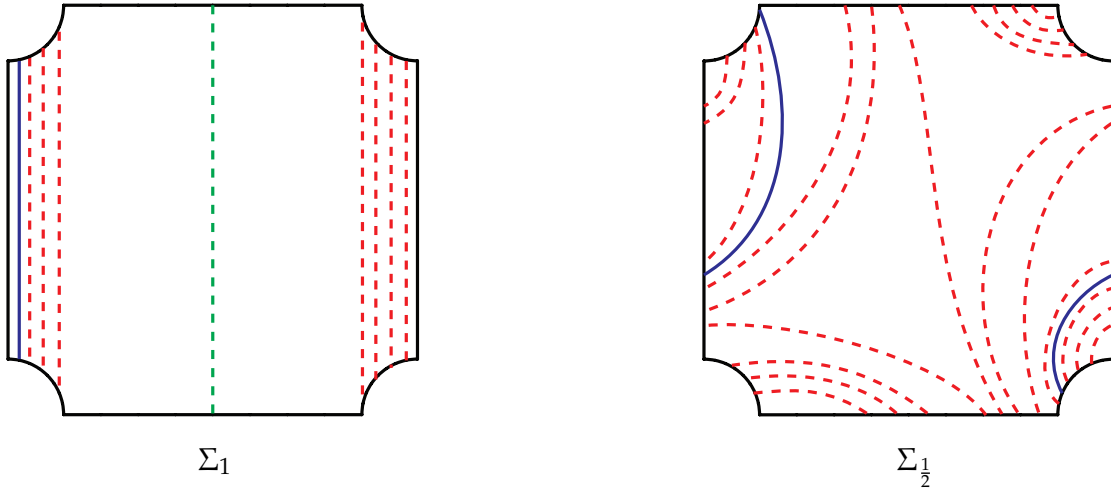


FIGURE 16. Σ_1 and $\Sigma_{\frac{1}{2}}$ in $C_n(7)$. The dotted lines are dividing curves and the blue lines are the intersections between an overtwisted disk and $\Sigma \times \{\frac{1}{2}, 1\}$

More precisely, there is no bypass passing through green, black, green dividing curves in order. Therefore, the only bypass that does not produce a boundary parallel arc is the one that straddles the green dividing curve. If the bypass straddles the green dividing curve, then attaching the bypass results in $\Sigma_{1/2}$ with $\Gamma_{1/2} = \{0, \frac{1}{n-2}, \frac{1}{n-3}\}$ where $\text{mult}(0) = 3$, $\text{mult}(\frac{1}{n-3}) = m - 4$ and $\text{mult}(\frac{1}{n-2}) = 1$. We can convert $\Gamma_{1/2}$ into $\{0, 1, \infty\}$ by acting on $\Sigma_{1/2}$ via ϕ_n^{-1} . Now we cut $C_n(s)$ along $\Sigma_{1/2}$ and obtain $\Sigma \times [0, 1]$ again. We relate $\Sigma \times \{i\}$ as Σ_i

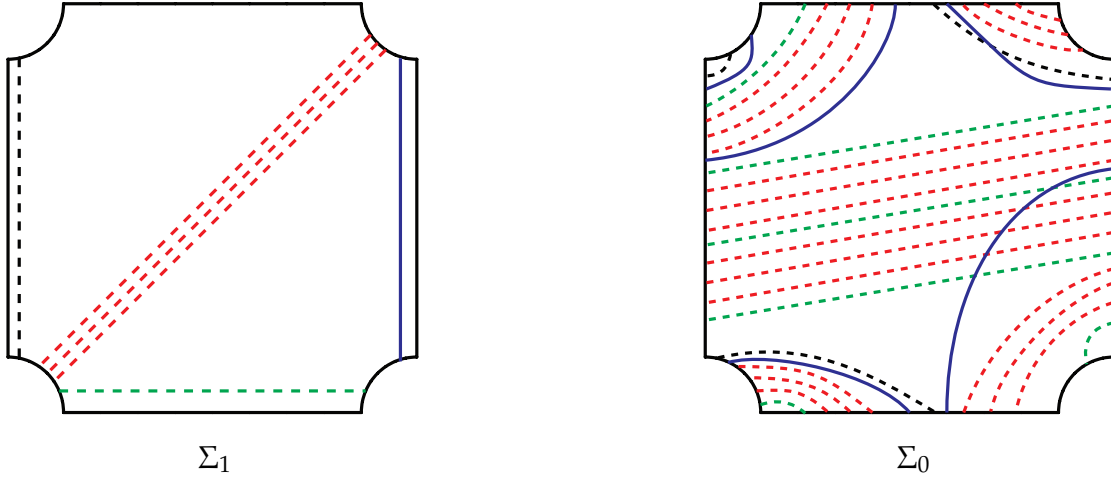


FIGURE 17. Σ_1 and Σ_0 in $C_n(\frac{5}{2})$. The dotted lines are dividing curves and the blue lines are $\alpha \times \{1\}$ and $\alpha \times \{0\}$

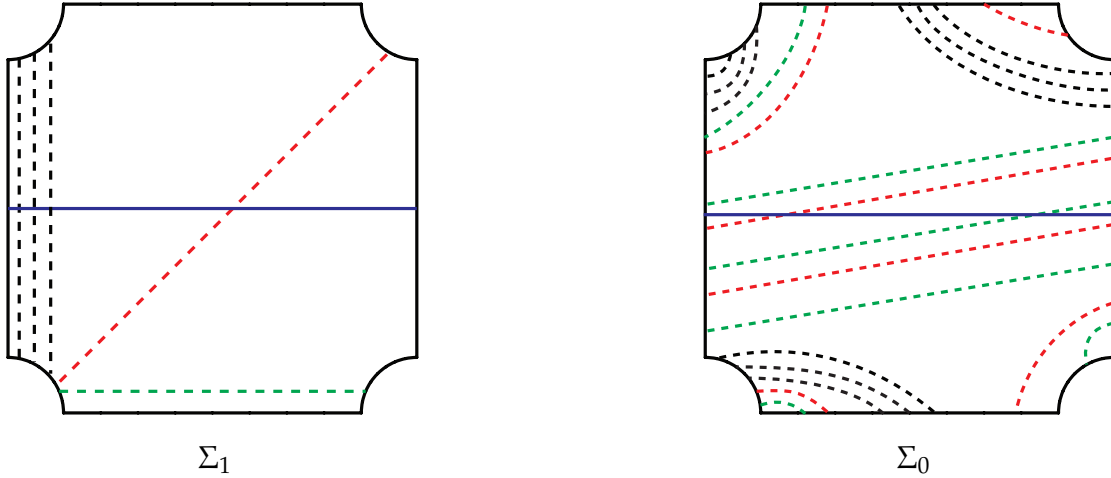


FIGURE 18. Σ_1 and Σ_0 in $C_n(\frac{5}{2})$. The dotted lines are dividing curves and the blue lines are $\gamma \times \{1\}$ and $\gamma \times \{0\}$

for $i = \{0, 1\}$. Then $\Gamma_1 = \{0, 1, \infty\}$ with $\text{mult}(0) = 1$, $\text{mult}(1) = m - 4$, $\text{mult}(\infty) = 3$. Take a closed curve γ with slope 0 and let $A_\gamma := \gamma \times [0, 1]$ be a properly embedded annulus in $\Sigma \times [0, 1]$. We perturb A_γ so that it is convex with Legendrian boundary and intersects $\Gamma_0 \cup \Gamma_1$ minimally, see Figure 18. Since $|\gamma \times \{1\} \cap \Gamma_1| = m - 1$ and $|\gamma \times \{0\} \cap \Gamma_0| = m - 3$, we can find a bypass whose attaching arc lies on Σ_1 by Theorem 2.5. Notice that we attach this bypass from the back. It is easy to check that any possible bypass attachment results in an isotopic copy of Σ that contains a boundary parallel dividing arc.

Now suppose $m = 3$. Since we assume $s \geq 2$, the only possible value of k is 1. In this case, there are exactly two possible bypass attachments on Σ_0 and both result in an isotopic copy of Σ containing boundary parallel dividing arc, see Figure 19. \square

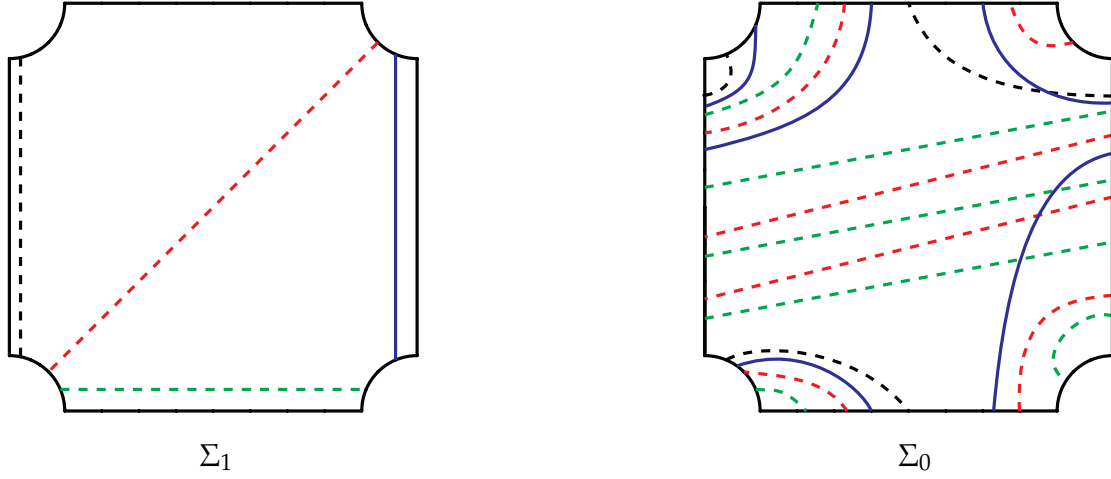


FIGURE 19. Σ_1 and Σ_0 in $C_n(3)$. The dotted lines are dividing curves and the blue lines are $\alpha \times \{1\}$ and $\alpha \times \{0\}$

Now we consider the case $s < 0$.

Proposition 4.15. *Suppose $s < 0$. Then there is an isotopic copy of Σ in $C_n(s)$ such that Γ_Σ contains a boundary parallel arc.*

Proof. Let $s = -\frac{m}{k}$ for a pair of relatively prime positive integers m, k . Then there are m properly embedded dividing arcs on Σ . We cut $C_n(s)$ along Σ to obtain a genus-2 handlebody $\Sigma \times [0, 1]$ and round edges to obtain a smooth convex boundary. Let Σ_i be $\Sigma \times \{i\}$ for $i = 0, 1$ and Γ_i the dividing set on Σ_i . Then $\Gamma_0 = \phi_n(\Gamma_1)$. After rounding the edges, the entire dividing set only contains closed curves, but we will keep calling the dividing curves that pass through $\partial\Sigma$ dividing arcs for convenience.

As in Proposition 4.14, the dividing arcs in Γ_i divides $\partial\Sigma_i$ into $2m$ intervals for $i = 0, 1$. The dividing curves on $\partial\Sigma \times [0, 1]$ connect the i -th interval on Σ_1 to the $(i + 2k - 1)$ -th interval (mod $2m$) on Σ_0 .

Suppose there is no boundary parallel dividing arc in Γ_i for $i = 0, 1$. By Proposition 4.12 and Proposition 4.13, we need to consider three cases.

(1) $m > 1$ and Γ_1 contains m arcs and one closed curve with slope ∞ : As in Proposition 4.14, let α be an arc on Σ_1 with slope ∞ that does not intersect Γ_1 . Let $D_\alpha := \alpha \times [0, 1]$ be a compressing disk for $\Sigma \times [0, 1]$. Perturb D_α so that its boundary does not intersect any dividing curve on $\partial\Sigma \times [0, 1]$. This results in a shift of the basepoints of α on Σ_0 by $(2k - 1)$ intervals following the positive orientation of $\partial\Sigma$. Thus ∂D_α only intersects the dividing curves in Γ_0 . We perturb D_α further so that it is convex with Legendrian boundary. We

can also assume that ∂D_α intersects Γ_0 minimally, so it will intersect the closed dividing curve exactly once. Also, this intersection point separates $\alpha \times \{0\}$ into two sides. On one side it intersects $|2k - 1|$ dividing arcs, and on the other side it intersects $|m + (2k - 1)|$ dividing arcs. Since the total number of intersection points is greater than 2, there is a bypass in D_α by Theorem 2.6. The difference between the number of intersections is:

$$d = |(m + 2k - 1) - (2k - 1)| = |m|.$$

Since we assume $m > 1$, we have $d \neq 1$ and the dividing curves in D_β cannot be nested as shown in the right drawing of Figure 14. This implies that there is always a bypass which does not straddle the closed dividing curve. After attaching this bypass, we obtain an isotopic copy of Σ containing a boundary parallel dividing arc.

(2) $m \geq 3$ and Γ_1 contains arcs with slope $\{0, 1, \infty\}$ where $\text{mult}(0) = \text{mult}(\infty) = 1$ and $\text{mult}(1) = m - 2$: Let β be an arc on Σ_1 with slopes ∞ that does not intersect Γ_1 and $D_\beta := \beta \times [0, 1]$ a compressing disk in $\Sigma \times [0, 1]$. We perturb D_β so that it is convex with Legendrian boundary and does not intersect dividing curves on $\partial \Sigma \times [0, 1]$. Since $\beta \times \{0\}$ intersects more than four dividing curves on Γ_0 , we can find a bypass in D_β whose attaching arc lies on $\beta \times \{0\}$ by Theorem 2.6. Notice that there is no bypass passing through green, black, green dividing curves in order. Therefore, the only bypass that does not produce a boundary parallel arc is the one that straddles the green dividing curve.

Suppose $m > 3$. If the bypass straddles the green dividing curve, then attaching the bypass results in $\Sigma_{1/2}$ with $\Gamma_{1/2} = \{0, \frac{1}{n-2}, \frac{1}{n-3}\}$ where $\text{mult}(0) = 3$, $\text{mult}(\frac{1}{n-3}) = m - 4$ and $\text{mult}(\frac{1}{n-2}) = 1$. We can convert $\Gamma_{1/2}$ into $\{0, 1, \infty\}$ by acting on $\Sigma_{1/2}$ via ϕ_n^{-1} . Now we cut $C_n(s)$ along $\Sigma_{1/2}$ and obtain $\Sigma \times [0, 1]$ again. We relabel $\Sigma \times \{i\}$ as Σ_i for $i = \{0, 1\}$. Then $\Gamma_1 = \{0, 1, \infty\}$ with $\text{mult}(0) = 1$, $\text{mult}(1) = m - 4$, $\text{mult}(\infty) = 3$. Take a closed curve γ with slope 0 and let $A_\gamma := \gamma \times [0, 1]$ be a properly embedded annulus in $\Sigma \times [0, 1]$. We perturb A_γ so that it is convex with Legendrian boundary and intersects $\Gamma_0 \cup \Gamma_1$ minimally, see Figure 18. Since $|\gamma \times \{1\} \cap \Gamma_1| = m - 1$ and $|\gamma \times \{0\} \cap \Gamma_0| = m - 3$, we can find a bypass whose attaching arc lies on Σ_1 by Theorem 2.5. Notice that we attach this bypass from the back. It is easy to check that any possible bypass attachment results in an isotopic copy of Σ that contains a boundary parallel dividing arc.

Now suppose $m = 3$. If the bypass straddles the green dividing curve, attaching the bypass results in an isotopic copy of Σ containing one closed dividing curve and three dividing arcs with slope 0. We can convert this into the dividing set containing one closed curve and three arcs with slope ∞ by acting on Σ via ϕ_n^{-1} . We already dealt with this in Case (1).

(3) $m = 1$ and there is one closed curve and one arc with slope ∞ : First, suppose $k > 1$. Then take an arc on Σ with slope 1 and let D_α be a disk in $\Sigma \times [0, 1]$ as shown in Figure 20. The number of intersection between D_α and $\Gamma_0 \cup \Gamma_1$ is $4k + 2$, so we can find a bypass in D_α by Theorem 2.6. If the bypass does not straddle the closed dividing curve, then attaching the bypass results in a boundary parallel dividing arc. If the bypass straddles the closed

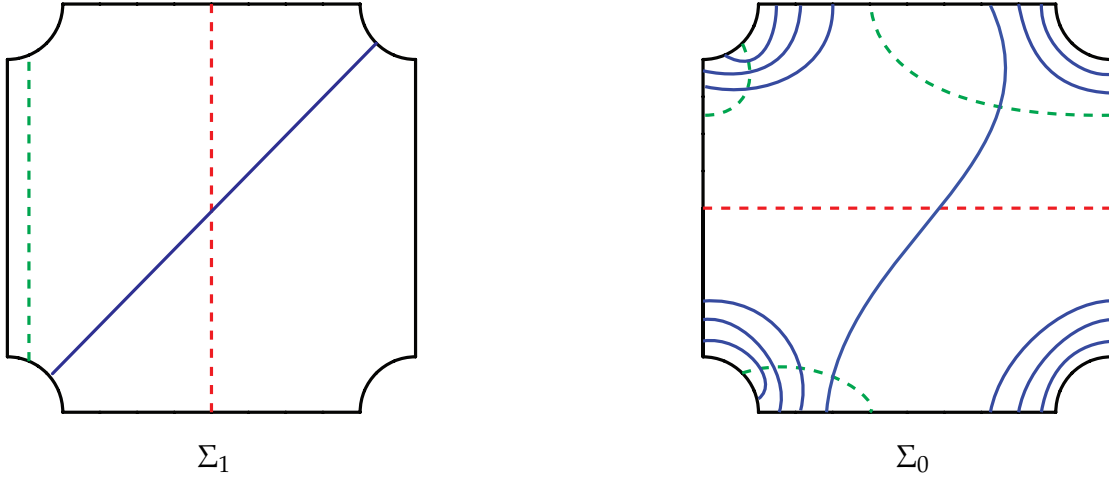


FIGURE 20. Σ_1 and Σ_0 in $C_n(-\frac{1}{2})$. The dotted lines are dividing curves and the blue lines are $\alpha \times \{1\}$ and $\alpha \times \{0\}$

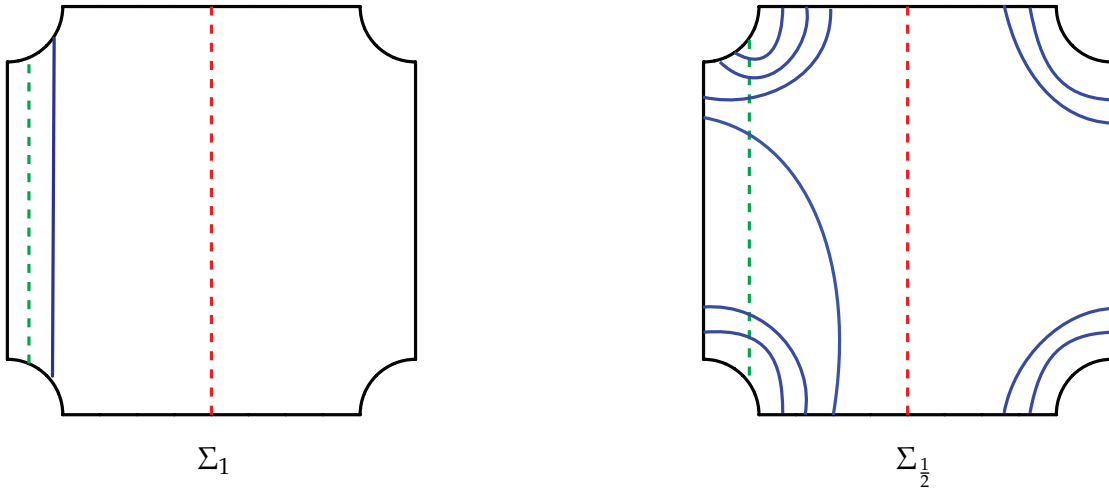


FIGURE 21. Σ_1 and $\Sigma_{\frac{1}{2}}$ in $C_n(-\frac{1}{2})$. The dotted lines are dividing curves and the blue lines are $\alpha \times \{1\}$ and $\alpha \times \{\frac{1}{2}\}$

dividing curve, then attaching the bypass results in $\Sigma_{1/2}$ with the dividing set identical to Γ_1 , see Figure 21. Now take an arc β with slope ∞ and let D_β be a compressing disk for $\Sigma \times [\frac{1}{2}, 1]$ as shown in Figure 21. Since the number of intersection between D_β and $\Gamma_{1/2} \cup \Gamma_1$ is $4k - 2$ and $k > 1$, we can find a bypass in D_β . Here, any possible bypass does not straddle the closed dividing curve, so attaching the bypass will result in a boundary parallel dividing arc.

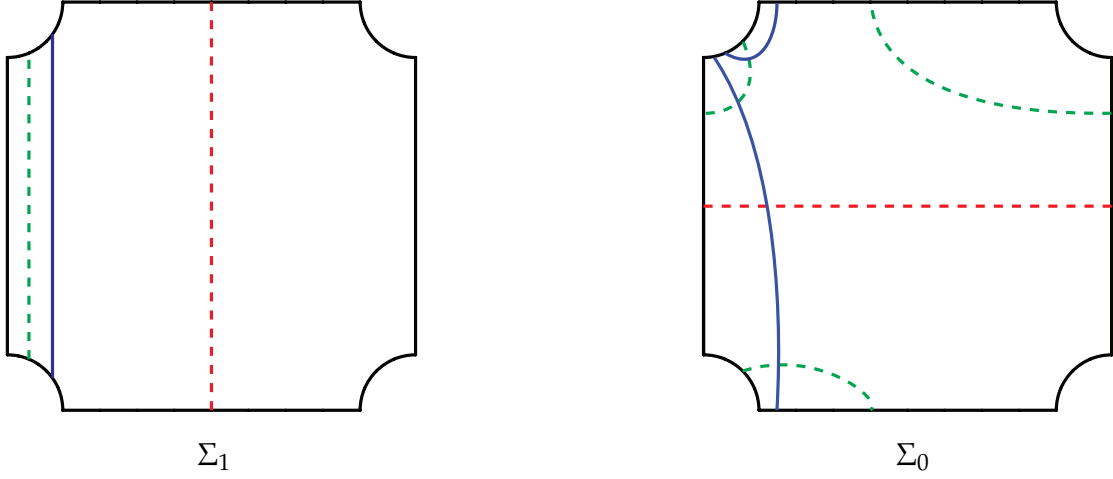


FIGURE 22. Σ_1 and Σ_0 in $C_n(-1)$. The dotted lines are dividing curves and the blue lines are $\alpha \times \{1\}$ and $\alpha \times \{0\}$

Now suppose $k = 1$. Take an arc on Σ with slope ∞ and let $D_\alpha = \alpha \times [0, 1]$ be a disk as shown in Figure 22. We call the closed dividing curve and the dividing arc on Σ_0 red and green dividing curves, respectively. Since the number of intersections between D_β and $\Gamma_0 \cup \Gamma_1$ is 4, there are two possible dividing sets for D_β . These two dividing sets provide two different bypasses. One bypass passes through red, green, green dividing curves in order. Attaching this bypass results in a boundary parallel dividing arc. The attaching arc of the other bypass does not lie on Σ_0 . The attaching arc only passes through two dividing curves on Σ_0 , see the top left drawing of Figure 23. By Theorem 2.7, we can rotate this bypass and obtain a new bypass such that its attaching arc lies on Σ_0 , see the top right drawing of Figure 23. Attaching this bypass results in a boundary parallel dividing arc. \square

4.4. Analyzing tight contact structures on $C_n(\frac{1}{k})$ for $k \leq 0$. In this subsection, we will prove Lemma 4.1, Lemma 4.2, 4.4 and 4.5. To do so, we need to prove Proposition 4.13 first.

Proof of Proposition 4.13. Since there is only one dividing arc, we know $s = \frac{1}{k}$ for $k \in \mathbb{Z}$ (we consider $\infty = \frac{1}{0}$). We cut $C_n(s)$ along Σ to obtain a genus-2 handlebody $\Sigma \times [0, 1]$. Let Σ_i be $\Sigma \times \{i\}$ for $i = 0, 1$ and Γ_i the dividing set on Σ_i . Then $\Gamma_0 = \phi_n(\Gamma_1)$. For $i = 0, 1$, the dividing arcs in Γ_i divides $\partial \Sigma_i$ into two intervals, which we will label by 1 and 2. The dividing curves on $\partial \Sigma \times [0, 1]$ connect the i -th interval on Σ_1 to the $(i - 2k - 1)$ -th interval (mod 2) on Σ_0 . Notice that $i - 2k - 1 \equiv i + 1 \pmod{2}$. By Proposition 4.9, we need to consider two cases.

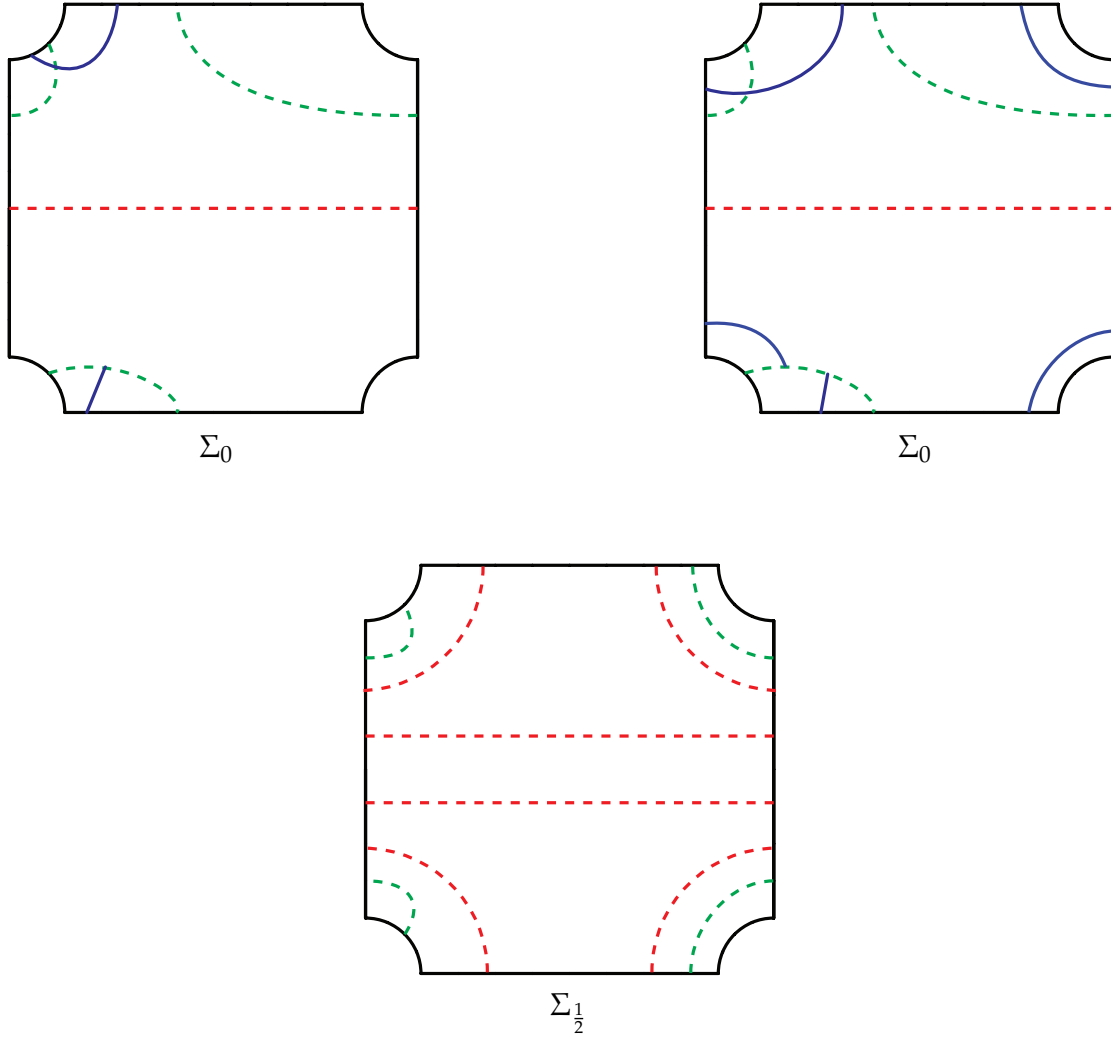


FIGURE 23. Top left: Σ_0 in $C_n(-1)$, before the bypass rotation. Top right: Σ_0 in $C_n(-1)$, after the bypass rotation. Bottom: $\Sigma_{\frac{1}{2}}$ in $C_n(-1)$, the result of the bypass attachment from the top right. The dotted lines are dividing curves and the blue lines are the attaching arcs of bypasses.

(1) Γ_1 consists of one closed curve and one arc with slope r : Recall from Proposition 4.12 that we calculated the slopes s_a^n and s_r^n of fixed points of ϕ_n and showed

$$0 < s_a^n < 1/2 \text{ and } 2 < s_r^n < \infty.$$

Before we cut $C_n(s)$ along Σ , we can change Γ by acting on Σ via $(\phi_n)^m$ for $m \in \mathbb{Z}$. Since $\phi_n(\infty) = 0$, we can assume r satisfies either

(a) $-\infty < r \leq 0$, or

(b) $s_a^n < r < 1 < s_r^n$.

For the case (a), we know $0 < \phi_n(r) < s_a^n$ since $\phi_n(\infty) = 0 < \phi_n(r)$ and s_a^n is the slope of the attracting fixed point. Assume r is not already 0. Let c be a closed curve on Σ with dividing slope $\phi_n(r)$ and $A_c := c \times [0, 1]$ be a properly embedded annulus in $\Sigma \times [0, 1]$. We perturb A_c so that it is convex with Legendrian boundary and intersects $\Gamma_0 \cup \Gamma_1$ minimally. Since $|c \times \{1\} \cap \Gamma_1| > 0$ and $|c \times \{0\} \cap \Gamma_0| = 0$, we can find a bypass whose attaching arc lies on Σ_1 by Theorem 2.5. We attach this bypass and keep track of dividing curves using Theorem 2.3. However, we should be careful according to Remark 2.4. First, we use the ordinary slope convention $\frac{q}{p} = \left(\frac{p}{q}\right)$ for Σ , so we should reverse the words “clockwise” and “anticlockwise”. Also, since the bypass is attached from the back, we should reverse the words “clockwise” and “anticlockwise” again. Therefore, the slope of the diving curves changes in a clockwise direction in the Farey graph. To summarize, attaching the bypass results in an isotopic copy of Σ with dividing slope r' that is clockwise of r , anticlockwise of $\phi_n(r)$ and closest to $\phi_n(r)$ with an edge to r . Simply, $r < r'$. We cut $C_n(s)$ again along this Σ and apply the same argument again. Repeat this procedure and we obtain an isotopic copy of Σ with slope 0 in the long run. By acting on Σ via ϕ_n^{-1} , we obtain Σ with dividing slope $\infty = \phi_n^{-1}(0)$.

Now consider the case (b). In this case, we know $0 < \phi_n(r) < r < 1$ since $\phi_n(r)$ is closer to s_a^n , the slope of the attracting fixed point of ϕ_n . Notice that the path in the Farey graph clockwise of r and anticlockwise of $\phi_n(r)$ contains 1 and ∞ . Let c be a closed curve on Σ with dividing slope $\phi_n(r)$ and $A_c := c \times [0, 1]$ be a properly embedded annulus in $\Sigma \times [0, 1]$. By the same argument in the case (a), we can find a bypass whose attaching arc lies on Σ_1 . Again, according to Remark 2.4 this bypass changes the slope of the diving curves in a clockwise direction in the Farey graph. To summarize, attaching the bypass results in an isotopic copy of Σ with dividing slope r' that is clockwise of r , anticlockwise of $\phi_n(r)$ and closest to $\phi_n(r)$ with an edge to r . We cut $C_n(s)$ again along this Σ and apply the same argument again. Since the path in the Farey graph clockwise of r and anticlockwise of $\phi_n(r)$ contains 1, we can obtain an isotopic copy of Σ with dividing slope 1 by repeating this procedure. It is still true that $s_a^n < 1 < s_r^n$, so we can apply the same argument (attaching the bypass to Σ_1) again. Since 1 and ∞ are connected by an edge in the Farey graph, we obtain Σ with dividing slope ∞ .

(2) Γ_1 contains a boundary parallel arc: In this case, Γ_1 may contain j boundary parallel closed curves and h essential closed curves, see Figure 24 for example, and we need to get rid of them. Observe that h is even. Let r be the slope of the essential dividing curves and α be an arc on Σ_1 with slope $\phi(r)$ that intersects the dividing arc twice, the closed boundary parallel dividing curves $2j$ times, and the essential closed curves $h|\phi(r) \cdot r|$ times, see the left drawing of Figure 24 for example. Observe that $|\phi(r) \cdot r| \geq 1$ since ϕ is pseudo-Anosov. Let $D_\alpha := \alpha \times [0, 1]$ be a compressing disk for $\Sigma \times [0, 1]$. Perturb D_α so that its boundary does not intersect any dividing curve on $\partial\Sigma \times [0, 1]$. This results in a shift of the basepoints of α on Σ_0 by $(2k + 1)$ intervals following the positive orientation

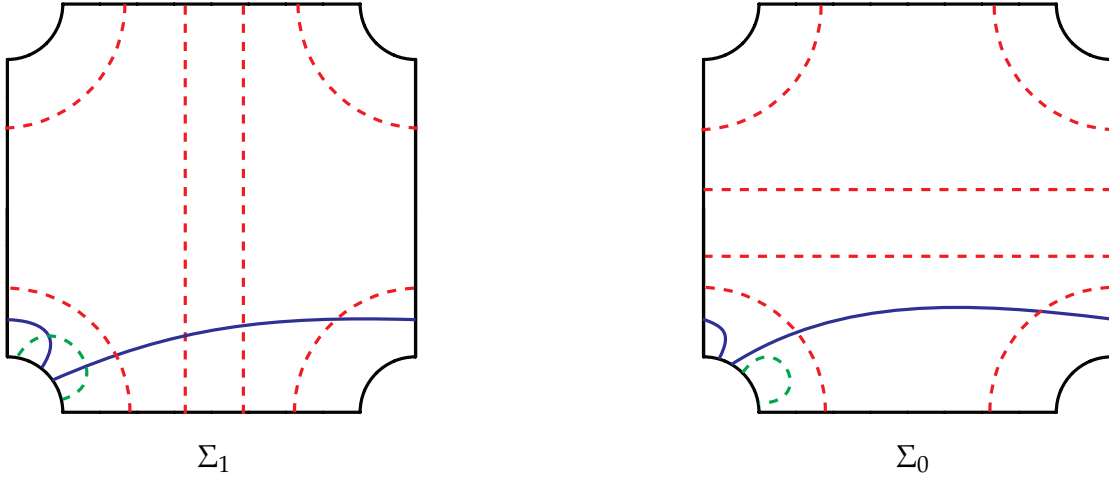


FIGURE 24. Σ_1 and Σ_0 in $C_n(\infty)$. The dotted lines are dividing curves and the blue lines are $\alpha \times \{1\}$ and $\alpha \times \{0\}$

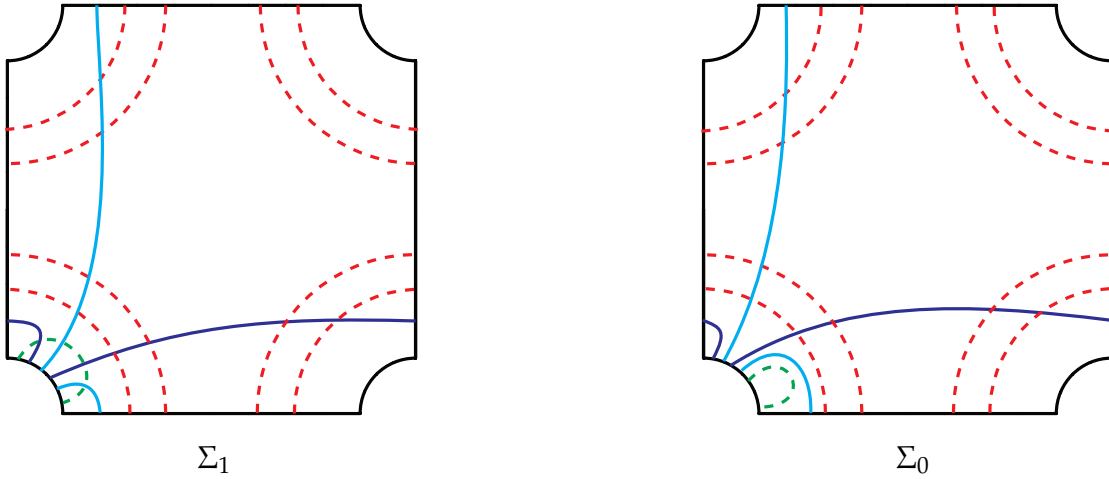


FIGURE 25. Σ_1 and Σ_0 in $C_n(\infty)$. The dotted lines are dividing curves, the blue lines are $\alpha \times \{1\}$ and $\alpha \times \{0\}$, and the sky blue lines are $\beta \times \{1\}$ and $\beta \times \{0\}$

of $\partial\Sigma$. We perturb D_α further so that it is convex with Legendrian boundary and $\alpha \times \{0\}$ intersects boundary parallel closed dividing curves $2j$ times as shown in the right drawing of Figure 24. To summarize, $\alpha \times \{1\}$ intersects at least $(2j + h + 2)$ dividing curves and $\alpha \times \{0\}$ intersects exactly $2j$ dividing curves. If $h \geq 2$, then we have $|\Gamma_1 \cap D_\alpha| - |\Gamma_0 \cap D_\alpha| \geq 4$, so we can find a bypass in D_α of which the attaching arc lies in $\alpha \times \{1\}$, see the right drawing of Figure 26 for example. By attaching this bypass, we

obtain an isotopic copy of Σ with 2 fewer dividing curves than the original one. We cut $C_n(s)$ along this new Σ and repeat this until h becomes 0.

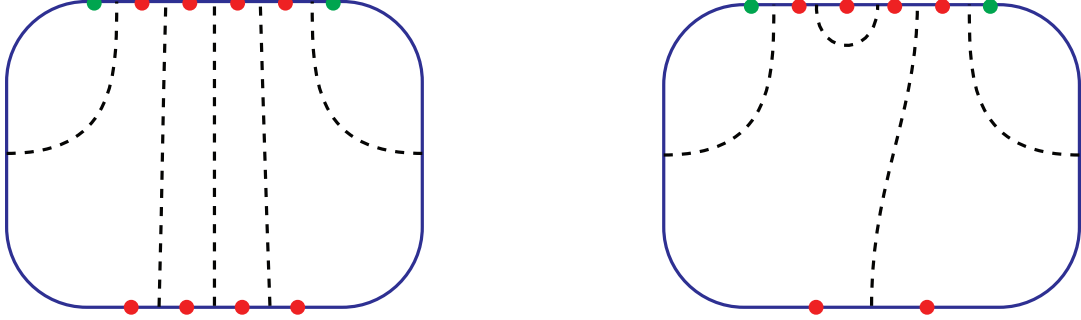


FIGURE 26. Dividing curves in D_α . Top sides: $\alpha \times \{1\}$. Bottom sides: $\alpha \times \{0\}$

Now we can assume $h = 0$ and $j > 0$. Here, we assume $s = \infty$. For other $s = \frac{1}{k}$, we attach a minimally twisting contact structure on $T = T^2 \times [0, 1]$ with dividing slopes ∞ and $\frac{1}{k}$ to $C_n(\frac{1}{k})$ and obtain $C_n(\infty)$. Then remove T at the end of the proof. Also, fix a sign of the bypass on Σ_1 to be negative. The argument will be the same for the positive case. Now we have

$$|\Gamma_1 \cap D_\alpha| - |\Gamma_0 \cap D_\alpha| = (2j + h + 2) - 2j = 2,$$

so there is a dividing set on D_α that does not provide a bypass of which the attaching arc lies in $\alpha \times \{1\}$ as shown in the left drawing of Figure 26. Observe that all other dividing sets on D_α (up to isotopy) will give a bypass of which the attaching arc lies in $\alpha \times \{1\}$. Now take an arc β on Σ_1 such that $\Sigma \setminus (\alpha \cup \beta)$ is a disk and β intersects Γ_1 $(2j + 2)$ times, see the left drawing of Figure 25 for example ($j = 2$). Let $D_\beta := \beta \times [0, 1]$ be a compressing disk for $\Sigma \times [0, 1]$. If we cut $\Sigma \times [0, 1]$ along D_α and D_β and round the edges, then we obtain a 3-ball B^3 with convex boundary. Since there is a unique tight contact structure on a 3-ball with a fixed characteristic foliation, tight contact structures on $\Sigma \times [0, 1]$ are completely determined by the dividing sets on D_α and D_β . As discussed above, all dividing sets on D_α (resp. D_β) contain a bypass of which the attaching arc lies in $\alpha \times \{1\}$ (resp. $\beta \times \{1\}$) except for the one shown in the left drawing of Figure 26. Therefore, in every tight contact structure on $\Sigma \times [0, 1]$, except for (possibly) one, there is a bypass for Σ_1 of which the attaching arc lies in $\alpha \times \{1\}$ or $\beta \times \{1\}$. As we observed above, attaching this bypass reduces the number of dividing curves. Denote the contact structure that might not contain such a bypass by ξ . By the Thurston–Bennequin inequality for convex surfaces [27], there is no bypass that decreases the number of dividing curves in an I -invariant neighborhood of a convex surface. Since the dividing curves on $\partial \Sigma \times [0, 1]$ are vertical, the contact structure ξ should be contactomorphic to an I -invariant neighborhood of Σ_1 .

Now consider a convex Giroux $\frac{1}{2}$ -torsion layer $(T^2 \times [0, 1], \xi_{j/2})$ with boundary slope ∞ . Since $T^2 \times [0, 1] = A \times S^1$, we cut $T^2 \times [0, 1]$ along A and obtain $A \times [0, 1]$. It is well

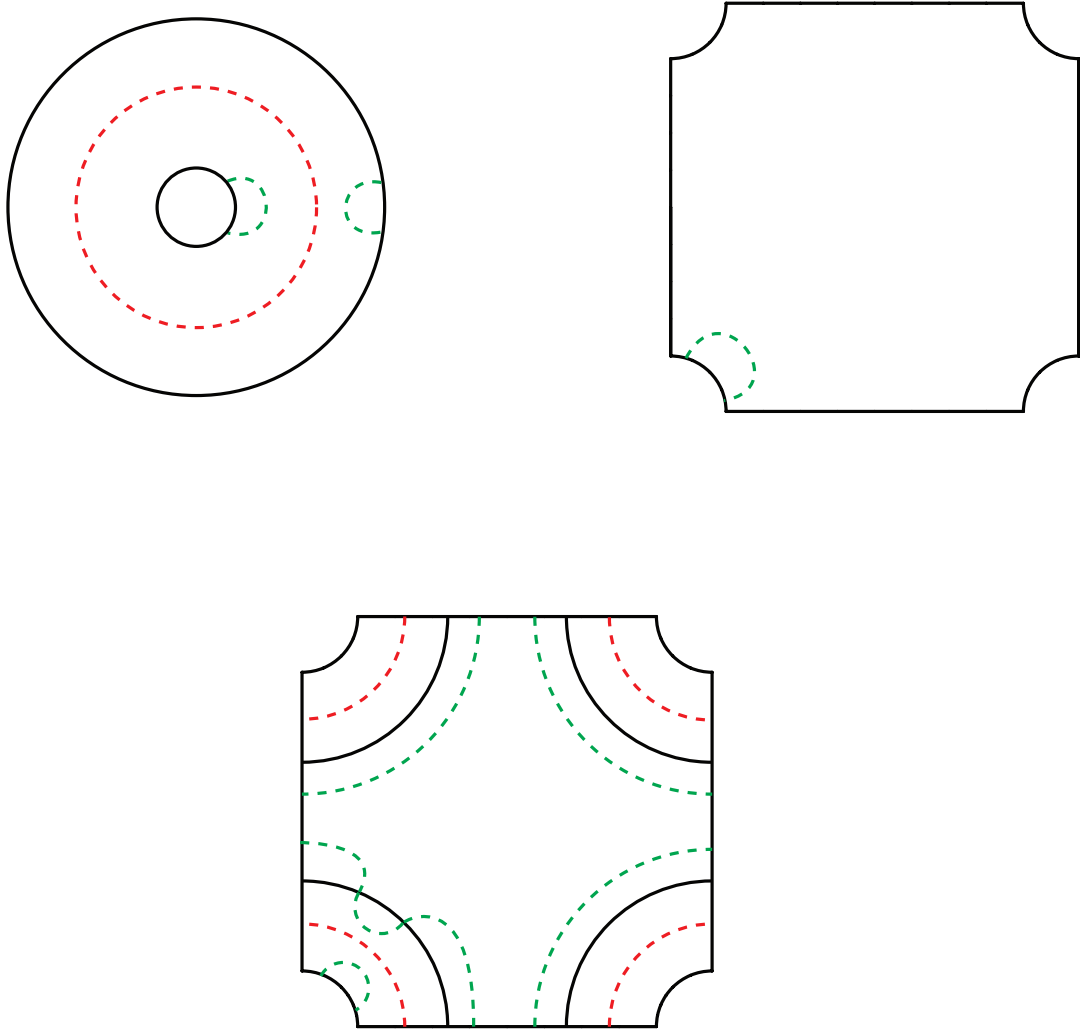


FIGURE 27. Top left: annulus in $T^2 \times [0, 1]$. Top right: Σ in $C_n(\infty)$. Bottom: Σ in $C_n(\infty)$ after gluing $T^2 \times [0, 1]$. The dotted lines are dividing curves.

known (c.f. [32, 46]) that there is a convex annulus A in $\xi_{j/2}$ with a boundary parallel dividing arc on each boundary component and $(j - 1)$ closed boundary parallel dividing curves, and $A \times [0, 1]$ is an I -invariant neighborhood, see the top left drawing of Figure 27 for Giroux 1-torsion ($j = 2$). We also consider a tight contact structure ξ_0 on $\Sigma \times [0, 1]$, an I -invariant neighborhood of a convex surface Σ with a single dividing arc without any other dividing curves, see the top right drawing of Figure 27. With appropriate choices of the signs of the bypasses on Σ and A , we obtain an I -invariant neighborhood of a convex surface with one dividing arc and j boundary parallel closed curves by gluing two contact structures ξ_0 and $\xi_{j/2}$, see the bottom drawing of Figure 27. Therefore, ξ

is contactomorphic to $\xi_{j/2} \cup \xi_0$. We glue the top and bottom of $(\Sigma \times [0, 1], \xi)$ using ϕ_n and obtain $C_n(s)$. Then it clearly contains Giroux $\frac{j}{2}$ -torsion. Thus we can exclude this case, and in any tight contact structure on $C_n(s)$ without boundary parallel half Giroux torsion, we can find a bypass for Σ_1 of which the attaching arc lies on $\alpha \times \{1\}$ or $\beta \times \{1\}$. By attaching this bypass we obtain an isotopic copy of Σ that contains 2 fewer dividing curves than Σ_1 . We cut $C_n(s)$ along this new Σ and repeat the argument until we obtain Σ without closed dividing curves. \square

According to Honda [31], there is a unique tight contact structure on $L(n, n-1)$ up to isotopy. We denote it by ξ_{std} . As explained in Section 4.1, K_2 can be considered as a knot in $L(n, n-1)$. Also, as shown in Figure 8, there is a Legendrian realization L of K_2 in $(L(n, n-1), \xi_{std})$ with $\text{tb} = 1$ and $\text{rot} = 0$ (which can be computed by using the formula from [40, Lemma 6.6]). We just have proved the following lemma.

Lemma 4.16. *There is a Legendrian representative L of K_2 in $(L(n, n-1), \xi_{std})$ such that $\text{tb}(L) = 1$ and $\text{rot}(L) = 0$.* \square

Now we are ready to prove the lemmas in Section 4.1. We begin with Lemma 4.1

Proof of Lemma 4.1. Since $r \in \mathcal{R}_+$ and $s \in \mathcal{S}(r)$, we know $s > 2$ and $s \notin (4, 5]$. By Proposition 4.14, we can find a bypass for $-\partial C_n(s)$ with slope 0. By Theorem 2.3, we can thicken $C_n(s)$ to $C_n(s')$ such that $s' > 2$ and $s' \notin (4, 5]$. If $s' \neq \infty$, we can find a bypass again by Proposition 4.14 and repeat this until we obtain $C_n(\infty)$. \square

Proof of Lemma 4.2. Again, after cutting $C_n(\infty)$ along Σ and rounding the edges, we obtain a genus-2 handlebody with convex boundary. Let Σ_i be $\Sigma \times \{i\}$ for $i = 0, 1$ and Γ_i the dividing set on Σ_i . Then $\Gamma_0 = \phi_n(\Gamma_1)$. The dividing arc in each Γ_i divides $\partial \Sigma_i$ into two intervals, which we will label by 1 and 2. The dividing curves on $\partial \Sigma \times [0, 1]$ connect the i -th interval on Σ_1 to the $(i-1)$ -th interval (mod 2) on Σ_0 . By Proposition 4.13, we need to consider two cases.

(1) Γ_1 consists of a boundary-parallel arc without any other dividing curves: First, we fix the sign of the bypass on Σ_1 to be negative. This will determine the signs of the regions of entire $\partial(\Sigma \times [0, 1])$. Also, the relative Euler class evaluated on Σ_1 is -2 . We observe that the dividing set on $\Sigma \times [0, 1]$ is a single closed curve parallel to $\partial \Sigma$. Thus we can choose two convex compressing disks for the handlebody of which the Legendrian boundaries intersect the dividing curve exactly twice, see Figure 28. Thus there is a unique (possibly) tight contact structure on this handlebody, and thus a unique (possibly) tight contact structure on $C_n(\infty)$, which we denote by ξ_{∞}^- . Now we change the sign of the bypass on Σ_1 to be positive. Then the relative Euler class evaluated on Σ_1 is 2. By repeating the same argument, we can show that there is a unique (possibly) tight contact structure on $C_n(\infty)$, which we denote by ξ_{∞}^+ .

It follows that any tight contact structure on $C_n(\infty)$ whose relative Euler class evaluated on Σ is ± 2 without boundary parallel half Giroux torsion is actually isotopic to ξ_{∞}^{\pm} ,

respectively. Now Let ξ_{-1}^- be a contact structure on $C_n(-1)$, the complement of a standard neighborhood of $S_-(S_-(L))$, where S_- is the negative stabilization operator and L is a Legendrian representative of K_2 in $(L(n, n-1), \xi_{std})$ with $\text{tb}(L) = 1$ and $\text{rot}(L) = 0$ according to Lemma 4.16. Also, denote by ξ_B^- the contact structure on a negative basic slice $B_-(\infty, -1)$. Honda [31] showed that any basic slice is universally tight, so ξ_B^- is universally tight. Also ξ_{-1}^- is universally tight according to Colin's gluing theorem [4] since the gluing surfaces only contain boundary parallel dividing arcs (this condition is called *well-groomed*). If we glue ξ_0^- and ξ_B^- along the boundary torus T_{-1} with dividing slope -1 , then we obtain a tight contact structure on $C_n(\infty)$ since T_{-1} is rotative and thus we can apply the gluing theorem for universally tight contact structures along a rotative torus [4, 34]. Clearly the relative Euler class evaluated on Σ in $\xi_0^- \cup \xi_B^-$ is -2 , so the tight contact structure $\xi_0^- \cup \xi_B^-$ is isotopic to ξ_∞^- . By the same argument, $\xi_0^+ \cup \xi_B^+$ is isotopic to ξ_∞^+ . Therefore, $(C_n(\infty), \xi_\infty^\pm)$ in fact thickens to $C_n(1)$.

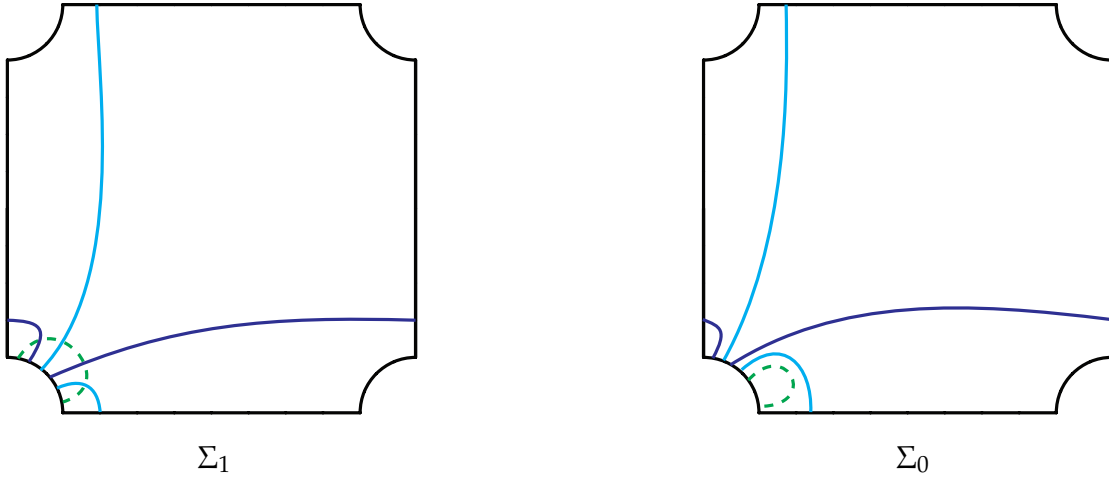


FIGURE 28. Σ_1 and Σ_0 in $C_n(\infty)$. The dotted lines are dividing curves, the blue lines are $\alpha \times \{1\}$ and $\alpha \times \{0\}$, and the sky blue lines are $\beta \times \{1\}$ and $\beta \times \{0\}$

(2) Γ_1 contains one arc and one closed curve with slope ∞ : In this case, the relative Euler class evaluated on Σ is 0. Fix the signs of the regions $\Sigma_1 \setminus \Gamma_1$. Take arcs α and β on Σ_1 with slopes ∞ and 0 as shown in the left drawing of Figure 29. Take compressing disks $D_\alpha = \alpha \times [0, 1]$ and $D_\beta = \beta \times [0, 1]$ for $\Sigma \times [0, 1]$. Perturb the disks so that their boundaries do not intersect any dividing curve on $\partial\Sigma \times [0, 1]$. This results in a shift of the basepoints of α and β on Σ_0 by -1 intervals following the positive orientation of $\partial\Sigma$. Then ∂D_α and ∂D_β intersect the dividing curves on $\partial(\Sigma \times [0, 1])$ exactly twice, respectively, as shown in Figure 29. Thus there is a unique (possibly) tight contact structure on this handlebody, and thus a unique (possibly) tight contact structure on $C_n(\infty)$. Now we change the sign of the regions $\Sigma_1 \setminus \Gamma_1$. By repeating the same argument, we can show that there is a unique

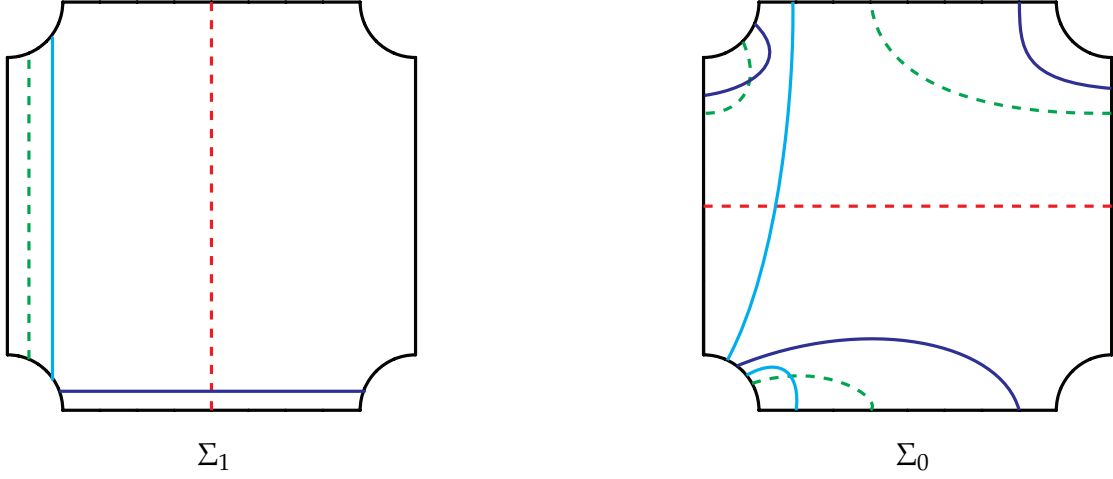


FIGURE 29. Σ_1 and Σ_0 in $C_n(\infty)$. The dotted lines are dividing curves, the blue lines are $\alpha \times \{1\}$ and $\alpha \times \{0\}$, and the sky blue lines are $\beta \times \{1\}$ and $\beta \times \{0\}$

(possibly) tight contact structure on $C_n(\infty)$. In total, there are at most two (possibly) tight contact structures on $C(\infty)$. \square

Remark 4.17. Since the dividing curves on Σ may have some boundary twisting for the case (2), there could be infinitely many tight contact structures on $C_n(\infty)$ if we fix the boundary pointwise.

Now we will prove Lemma 4.4 and 4.5. The argument will be similar to the proof of [7, Lemma 3.1 and 3.4]. However, since ϕ_n is right veering, whereas the monodromy of the figure-eight knot is not, the maximal slope to which $C_n(s)$ can thicken is different.

Proof of Lemma 4.4 and 4.5. Since $r \in \mathbb{Q}_-$, $s \in \mathcal{S}(r)$ and $s \neq 0$, we know $s < 0$. Let $k \in \mathbb{N}$ such that $-\frac{1}{k-1} < s \leq -\frac{1}{k}$. Suppose $s \neq -\frac{1}{k}$. Then by Proposition 4.15 we can find a bypass for $-\partial C_n(s)$ with slope 0 and we can thicken $C_n(s)$ to $C_n(s')$ where $s < s' \leq -\frac{1}{k}$. Thus we can find a bypass again by Proposition 4.15 and repeat this until we obtain $C_n(-\frac{1}{k})$. Let Γ_Σ be a dividing set for Σ in $C_n(-\frac{1}{k})$. By Proposition 4.13, we need to consider two cases.

(1) Γ_Σ contains one boundary parallel arc without any other dividing curves: First, we fix the sign of the bypass on Σ to be negative. Then the relative Euler class evaluated on Σ is -2 . After cutting $C_n(-\frac{1}{k})$ along Σ and rounding the edges, we obtain $\Sigma \times [0, 1]$ with a smooth convex boundary. Also, the dividing set consists of a single closed curve parallel to $\partial \Sigma$. By choosing convex compressing disks for this handlebody whose Legendrian boundaries intersect the dividing curve exactly twice as shown in Figure 28, we see that there is a unique (possibly) tight contact structure on this handlebody, and thus a unique (possibly) tight contact structure on $C_n(-\frac{1}{k})$, which we denote by $\xi_{-1/k}^-$.

It follows that any tight contact structure on $C_n(-\frac{1}{k})$ whose relative Euler class evaluated on Σ is -2 without boundary parallel half Giroux torsion is actually isotopic to $\xi_{-1/k}^-$. Hence the complement of a standard neighborhood of $S_-(S_-(L))$ in $(L(n, n-1), \xi_{std})$ is isotopic to ξ_{-1}^- , where S_- is the negative stabilization operator and L is a Legendrian representative of K_2 from Lemma 4.16. Therefore, $(C_n(-1), \xi_{-1}^-)$ in fact thickens to $C_n(1)$, and $C_n(-1) = T_- \cup C(\infty)$, where $T_- = B_-(-1, 0) \cup B_-(0, 1)$ is a union of two negative basic slices with dividing slopes $s_0 = -1$ and $s_1 = 1$. We can further decompose T_- into $T_-^k \cup B_-(-\frac{1}{k}, 0) \cup B_-(0, 1)$, where T_-^k is a minimally twisting contact $T^2 \times [0, 1]$ with dividing slopes $s_0 = -1$ and $s_1 = -\frac{1}{k}$. Hence we obtain a tight contact structure on $C_n(-\frac{1}{k}) = B_-(-\frac{1}{k}, 0) \cup B_-(0, 1) \cup C(1)$. It is straightforward to check that the relative Euler class evaluated on Σ in this $C_n(-\frac{1}{k})$ is -2 , so this contact structure is isotopic to $\xi_{-1/k}^-$. Therefore, $(C_n(-\frac{1}{k}), \xi_{-1/k}^-)$ also thickens to $C_n(1)$ for all $k \in \mathbb{N}$.

Next, change the signs of the regions of Σ so that the sign of the bypass is positive. In this case, the relative Euler class evaluated on Σ is 2 . After repeating the above argument, we get a unique tight contact structure under these conditions, which we denote by $\xi_{-1/k}^+$. Similarly, we can build the tight contact structures isotopic to $(C_n(-\frac{1}{k}), \xi_{-1/k}^+)$ that thicken to $C_n(1)$.

The above arguments show that these tight contact structures on $C_n(-\frac{1}{k})$ are determined by the sign of the bypass on Σ , which is in turn determined by the sign on the stacks of basic slices $B_{\pm}(-\frac{1}{k}, 0) \cup B_{\pm}(0, 1)$, and are thus independent of the tight contact structure on $C_n(1)$.

(2) Γ_{Σ} contains one closed curve and one arc with slope ∞ : In this case, the relative Euler class evaluated on Σ is 0 . Fix the signs of the regions $\Sigma \setminus \Gamma_{\Sigma}$. We showed in the proof of Proposition 4.15 that there exists an isotopic copy of Σ in $C_n(-\frac{1}{k})$ with one boundary parallel dividing arc, one closed boundary parallel dividing curve and perhaps two closed essential curves, see the bottom drawing of Figure 23 for example. As in the proof of Proposition 4.13, we can remove the closed essential dividing curves and hence we can assume Γ_{Σ} consists of one boundary parallel arc and one boundary parallel closed curve. This implies that the dividing set of $\partial(\Sigma \times [0, 1])$ consists of exactly three dividing curves parallel to $\partial\Sigma$. By Cofer [2, Section 3], there exist two tight contact structures on this $\Sigma \times [0, 1]$ (with a fixed characteristic foliation). Thus there exist at most two tight contact structures on $C_n(-\frac{1}{k})$.

According to the proof of Proposition 4.15, it is clear that one of these contact structures contains a boundary parallel half Giroux torsion layer. By repeating the same argument with the opposite signs on the regions on $\Sigma \setminus \Gamma_{\Sigma}$, we see that there are at most two tight contact structures on $C_n(-\frac{1}{k})$ without boundary parallel half Giroux torsion when the relative Euler class evaluated on Σ is 0 , and that these contact structures are completely determined by the sign of the bypass on Σ . Denote these contact structures by $(C_n(-\frac{1}{k}), \xi_{-1/k}^{\pm})$.

It follows that any tight contact structure on $C_n(-\frac{1}{k})$ whose relative Euler class evaluated on Σ is 0 without boundary parallel half Giroux torsion is actually isotopic (fixing boundary setwise) to either $\xi'_{-1/k}^+$ or $\xi'_{-1/k}^-$. Thus according to Lemma 4.16, the complement of a standard neighborhood of $S_+(S_-(L))$ (*resp.* $S_-(S_+(L))$) in $(L(n, n-1), \xi_{std})$ is isotopic to ξ'_{-1}^+ (*resp.* ξ'_{-1}^-). Therefore, $(C_n(-1), \xi'_{-1}^\pm)$ in fact thickens to $C_n(1)$, and $C_n(-1) = T'_\pm \cup C_n(1)$, where $T'_\pm = B_\pm(-1, 0) \cup B_\mp(0, 1)$ is a union of two negative basic slices with dividing slopes $s_0 = -1$ and $s_1 = 1$. We further decompose T'_\pm into $T'^k_\pm \cup B_\pm(-\frac{1}{k}, 0) \cup B_\mp(0, 1)$, where T'^k_\pm is a minimally twisting contact $T^2 \times [0, 1]$ with dividing slopes $s_0 = -1$ and $s_1 = -\frac{1}{k}$. Hence we obtain tight contact structures on $C_n(-\frac{1}{k}) = B_\pm(-\frac{1}{k}, 0) \cup B_\mp(0, 1) \cup C_n(1)$. It is straightforward to check that the relative Euler class evaluated on Σ is 0 and the sign of the bypass is \pm , so these contact structures are isotopic (fixing boundary setwise) to $\xi'_{-1/k}^\pm$. Therefore, $(C_n(-\frac{1}{k}), \xi'_{-1/k}^\pm)$ also thickens to $C_n(1)$ for all $k \in \mathbb{N}$.

The above arguments show that these tight contact structures on $C_n(-\frac{1}{k})$ are determined by the sign of the bypass on Σ , which is in turn determined by the sign on the stacks of basic slices $B_\pm(-\frac{1}{k}, 0) \cup B_\mp(0, 1)$, and are thus independent of the tight contact structure on $C_n(1)$. \square

4.5. Tight contact structures on a solid torus. In this subsection, we prove Lemma 4.7 by counting the number of tight contact structures on $N_r(\infty)$ and $N_r(1)$.

Proof of Lemma 4.7. By Proposition 2.13, there exist $\Phi(r)$ tight contact structures on $N_r(\infty)$.

Now we consider $N_r(1)$. Let $r = \frac{p}{q}$ and $r \neq 1$. We can change the coordinates of $\partial N_r(1)$ by the matrix

$$\begin{pmatrix} 0 & 1 \\ -1 & 1 \end{pmatrix}.$$

Then the dividing slope of $N_r(1)$ will become ∞ and the meridional slope will become $\frac{q}{q-p} = \frac{1}{1-r}$ (recall that we use the slope convention $(\frac{p}{q}) = \frac{p}{q}$ for a solid torus, see Remark 2.4). Therefore, there are $\Phi(\frac{1}{1-r}) = \Psi(r)$ tight contact structures on $N_r(1)$. \square

5. FILLABILITY AND VIRTUAL OVERTWISTEDNESS

In this section, we will prove Theorem 1.6 and Theorem 1.7. We begin with the fillability of tight contact structures on $M(n, r)$.

Proof of Theorem 1.6. First, we consider the tight contact structures counted by Φ . In [13], tight contact structures on $S_n^3(T_{2,3})$ are classified and it is shown that every tight contact structure on $S_n^3(T_{2,3})$ is Stein fillable for $n \geq 5$. Recall from Section 3 that the tight contact structures counted by Φ can be constructed from the surgery diagram shown in Figure 10, which can be considered as a result of Legendrian surgeries on the knots in some tight contact structure on $S_n^3(T_{2,3})$. Since Legendrian surgery preserves Stein fillability, all tight contact structures counted by Φ for $n \geq 5$ are Stein fillable.

Next we consider the tight contact structures counted by Ψ . Observe that there is a unique tight contact structure on $M(n, 2)$ counted by Ψ and denote it by $(M(n, 2), \xi_2)$. We claim that $(M(n, 2), \xi_2)$ is Stein fillable and show that any tight contact structure on $M(n, r)$ for $r > 2$ counted by Ψ is obtained by some negative contact surgery on some Legendrian knot in $(M(n, 2), \xi_2)$. Since negative contact surgery preserves Stein fillability, these will complete the proof.

Lemma 4.5 and the proof of Theorem 4.8 implies that any contact structure on $M(n, r)$ for $n \geq 2$ and $r \geq 2$ counted by Ψ can be obtained by a positive contact surgery on a Legendrian push-off of the binding of an open book decomposition of $(L(n, n-1), \xi_{std})$, the unique tight contact structure on $L(n, n-1)$. This in fact implies that any tight contact structure on $M(n, r)$ for $r > 2$ counted by Ψ can be obtained by some negative contact surgery on some Legendrian knot in $(M(n, 2), \xi_2)$.

To be more precise, the open book is shown in the left drawing of Figure 30 where the monodromy of the open book is $\phi_n = D_\alpha D_\beta D_\alpha^{n-1}$, where D_α is a positive Dehn twist about α . This positive contact surgery is equivalent to an inadmissible transverse 2-surgery on the binding of the open book followed by a negative contact surgery on a Legendrian push-off of the surgery dual knot (*c.f.* [6]). Also this inadmissible transverse 2-surgery yields $(M(n, 2), \xi_2)$.

By applying an algorithm in [6] that converts the result of an inadmissible transverse surgery into an open book decomposition, we obtain an open book decomposition for $(M(n, 2), \xi_2)$ as shown in the right drawing of Figure 30 where the monodromy is

$$\tilde{\phi}_n = D_\alpha D_\beta D_\alpha^{n-1} D_\gamma^{-1} \Delta$$

and Δ is the composition of positive Dehn twists about each boundary component. Korkmaz and Ozbagci [38] provided factorizations of Δ . In particular, they showed

$$\Delta = D_\alpha^{-2} D_\gamma D_\delta D_\sigma = D_\gamma D_\alpha^{-2} D_\delta D_\sigma$$

where δ, σ are some simple closed curves on the page. The second equality holds since α and γ are disjoint. Now we have

$$\begin{aligned} \tilde{\phi}_n &= D_\alpha D_\beta D_\alpha^{n-1} D_\gamma^{-1} \Delta \\ &= D_\alpha D_\beta D_\alpha^{n-1} D_\gamma^{-1} D_\gamma D_\alpha^{-2} D_\delta D_\sigma \\ &= D_\alpha D_\beta D_\alpha^{n-3} D_\delta D_\sigma. \end{aligned}$$

Since $n \geq 5$, there is a factorization of $\phi_n \Delta$ which is a product of positive Dehn twists. Thus $(M(n, 2), \xi_2)$ is Stein fillable. \square

Lastly, we will consider the virtual overtwistedness of tight contact structures on $M(n, r)$.

Proof of Theorem 1.7. First, as shown in Figure 1, $M(n, r)$ can be obtained by r -surgery on K_2 in $L(n, n-1)$ and the surgery dual knot K_* represents a nontrivial element in $\pi_1(M(n, r))$. Thus there is a cover of $M(n, r)$ that unwraps K_* . Let N be a neighborhood of K_* . By Honda [31, Proposition 5.1.(2)], if ξ is a virtually overtwisted contact structure

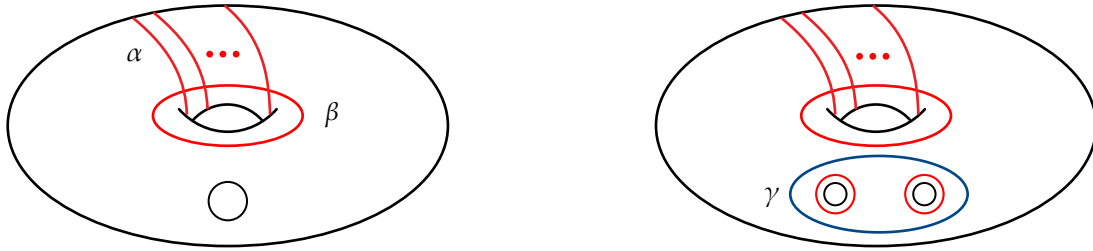


FIGURE 30. Left: an open book decomposition for $(L(n, n-1), \xi_{std})$. Right: an open book decomposition for $(M(n, 2), \xi_2)$ counted by Ψ . The red curves represent positive Dehn twists and the blue curve represents a negative Dehn twist.

on N , then any cover of (N, ξ) contains an overtwisted disk. Thus if (N, ξ) is virtually overtwisted, then there is an overtwisted cover of (N, ξ) that embeds into some cover of $M(n, r)$.

Now according to the proof of Theorem 4.8, the tight contact structures counted by Ψ can be decomposed into $C(1)$ and $N_r(1)$. By Honda [31, Proposition 5.1.(2)], there are at most two universally tight contact structures on $N_r(1)$. Thus for any $r \in \mathcal{R}_+ \cup \mathbb{Q}_-$, there are at most two universally tight contact structures on $M(n, r)$ counted by Ψ and all others are virtually overtwisted. Also, the tight contact structures counted by Φ can be decomposed into $C(\infty)$ and $N_r(\infty)$. By Honda [31, Proposition 5.1.(2)] again, there are at most two universally tight contact structures on $N_r(\infty)$. Since there are two tight contact structures on $C_n(\infty)$ counted by Φ , there are at most four universally tight contact structures on $M(n, r)$ for $r \in \mathcal{R}_+$ counted by Φ , and all others are virtually overtwisted. \square

REFERENCES

- [1] Kenneth Baker and John Etnyre. Rational linking and contact geometry. In *Perspectives in analysis, geometry, and topology*, volume 296 of *Progr. Math.*, pages 19–37. Birkhäuser/Springer, New York, 2012.
- [2] Tanya Cofer. A class of tight contact structures on $\Sigma_2 \times I$. *Algebr. Geom. Topol.*, 4:961–1011, 2004.
- [3] Vincent Colin. Chirurgies d’indice un et isotopies de sphères dans les variétés de contact tendues. *C. R. Acad. Sci. Paris Sér. I Math.*, 324(6):659–663, 1997.
- [4] Vincent Colin. Recollement de variétés de contact tendues. *Bull. Soc. Math. France*, 127(1):43–69, 1999.
- [5] Vincent Colin, Emmanuel Giroux, and Ko Honda. Finitude homotopique et isotopique des structures de contact tendues. *Publ. Math. Inst. Hautes Études Sci.*, (109):245–293, 2009.
- [6] James Conway. Transverse surgery on knots in contact 3-manifolds. *Trans. Amer. Math. Soc.*, 372(3):1671–1707, 2019.
- [7] James Conway and Hyunki Min. Classification of tight contact structures on surgeries on the figure-eight knot. *Geom. Topol.*, 24(3):1457–1517, 2020.
- [8] Fan Ding and Hansjörg Geiges. A Legendrian surgery presentation of contact 3-manifolds. *Math. Proc. Cambridge Philos. Soc.*, 136(3):583–598, 2004.

- [9] Fan Ding and Hansjörg Geiges. A unique decomposition theorem for tight contact 3-manifolds. *Enseign. Math. (2)*, 53(3-4):333–345, 2007.
- [10] Fan Ding, Hansjörg Geiges, and András I. Stipsicz. Surgery diagrams for contact 3-manifolds. *Turkish J. Math.*, 28(1):41–74, 2004.
- [11] Y. Eliashberg. Classification of overtwisted contact structures on 3-manifolds. *Invent. Math.*, 98(3):623–637, 1989.
- [12] Yakov Eliashberg. Contact 3-manifolds twenty years since J. Martinet’s work. *Ann. Inst. Fourier (Grenoble)*, 42(1-2):165–192, 1992.
- [13] John B. Etnyre, Hyunki Min, and Bülent Tosun. Tight surgeries on torus knots. In preparation.
- [14] John B. Etnyre. Convex surfaces in contact geometry: Class notes.
- [15] John B. Etnyre. Tight contact structures on lens spaces. *Commun. Contemp. Math.*, 2(4):559–577, 2000.
- [16] John B. Etnyre. Introductory lectures on contact geometry. *Proc. Sympos. Pure Math.*, 71:81–107, 2003.
- [17] John B. Etnyre. Legendrian and transversal knots. In *Handbook of knot theory*, pages 105–185. Elsevier B. V., Amsterdam, 2005.
- [18] John B. Etnyre. Lectures on open book decompositions and contact structures. In *Floer homology, gauge theory, and low-dimensional topology*, volume 5 of *Clay Math. Proc.*, pages 103–141. Amer. Math. Soc., Providence, RI, 2006.
- [19] John B. Etnyre and Ko Honda. Knots and contact geometry. I. Torus knots and the figure eight knot. *J. Symplectic Geom.*, 1(1):63–120, 2001.
- [20] John B. Etnyre and Ko Honda. On the nonexistence of tight contact structures. *Ann. of Math. (2)*, 153(3):749–766, 2001.
- [21] David Gabai, Robert Meyerhoff, and Peter Milley. Minimum volume cusped hyperbolic three-manifolds. *J. Amer. Math. Soc.*, 22(4):1157–1215, 2009.
- [22] Paolo Ghiggini. Ozsváth-Szabó invariants and fillability of contact structures. *Math. Z.*, 253(1):159–175, 2006.
- [23] Paolo Ghiggini, Paolo Lisca, and András I. Stipsicz. Tight contact structures on some small Seifert fibered 3-manifolds. *Amer. J. Math.*, 129(5):1403–1447, 2007.
- [24] Paolo Ghiggini and Stephan Schönenberger. On the classification of tight contact structures. In *Topology and geometry of manifolds (Athens, GA, 2001)*, volume 71 of *Proc. Sympos. Pure Math.*, pages 121–151. Amer. Math. Soc., Providence, RI, 2003.
- [25] Emmanuel Giroux. Une infinité de structures de contact tendues sur une infinité de variétés. *Invent. Math.*, 135(3):789–802, 1999.
- [26] Emmanuel Giroux. Structures de contact en dimension trois et bifurcations des feuilletages de surfaces. *Invent. Math.*, 141(3):615–689, 2000.
- [27] Emmanuel Giroux. Structures de contact sur les variétés fibrées en cercles audessus d’une surface. *Comment. Math. Helv.*, 76(2):218–262, 2001.
- [28] Marco Golla. Ozsváth-Szabó invariants of contact surgeries. *Geom. Topol.*, 19(1):171–235, 2015.
- [29] Robert E. Gompf. Handlebody construction of Stein surfaces. *Ann. of Math. (2)*, 148(2):619–693, 1998.
- [30] Craig D. Hodgson, G. Robert Meyerhoff, and Jeffrey R. Weeks. Surgeries on the Whitehead link yield geometrically similar manifolds. *Topology ’90 (Columbus, OH, 1990)*, 1:195–206, 1992.
- [31] Ko Honda. On the classification of tight contact structures. I. *Geom. Topol.*, 4:309–368, 2000.
- [32] Ko Honda. On the classification of tight contact structures. II. *J. Differential Geom.*, 55(1):83–143, 2000.
- [33] Ko Honda. Gluing tight contact structures. *Duke Math. J.*, 115(3):435–478, 2002.
- [34] Ko Honda, William H. Kazez, and Gordana Matić. Convex decomposition theory. *Int. Math. Res. Not.*, (2):55–88, 2002.
- [35] Ko Honda, William H. Kazez, and Gordana Matić. Tight contact structures on fibered hyperbolic 3-manifolds. *J. Differential Geom.*, 64(2):305–358, 2003.

- [36] Ko Honda, William H. Kazez, and Gordana Matic. Pinwheels and bypasses. *Algebr. Geom. Topol.*, 5:769–784, 2005.
- [37] Yutaka Kanda. The classification of tight contact structures on the 3-torus. *Comm. Anal. Geom.*, 5(3):413–438, 1997.
- [38] Mustafa Korkmaz and Burak Ozbagci. On sections of elliptic fibrations. *Michigan Math. J.*, 56(1):77–87, 2008.
- [39] Youlin Li and Zhongtao Wu. A bound for rational Thurston-Bennequin invariants. *Geom. Dedicata*, 200:371–383, 2019.
- [40] Paolo Lisca, Peter Ozsváth, András I. Stipsicz, and Zoltán Szabó. Heegaard Floer invariants of Legendrian knots in contact three-manifolds. *J. Eur. Math. Soc. (JEMS)*, 11(6):1307–1363, 2009.
- [41] Paolo Lisca and András I. Stipsicz. Ozsváth-Szabó invariants and tight contact three-manifolds. I. *Geom. Topol.*, 8:925–945, 2004.
- [42] Paolo Lisca and András I. Stipsicz. Ozsváth-Szabó invariants and tight contact 3-manifolds. III. *J. Symplectic Geom.*, 5(4):357–384, 2007.
- [43] Yajing Liu. L -space surgeries on links. *Quantum Topol.*, 8(3):505–570, 2017.
- [44] Thomas E. Mark and Bülent Tosun. Naturality of Heegaard Floer invariants under positive rational contact surgery. *J. Differential Geom.*, 110(2):281–344, 2018.
- [45] Bruno Martelli. Dehn surgery on the minimally twisted seven-chain link. *Comm. Anal. Geom.*, 29(7):1597–1641, 2021.
- [46] Daniel V. Mathews. Sutured TQFT, torsion and tori. *Internat. J. Math.*, 24(5):1350039, 35, 2013.
- [47] Kanji Morimoto. Genus one fibered knots in lens spaces. *J. Math. Soc. Japan*, 41(1):81–96, 1989.
- [48] Peter Ozsváth and Zoltán Szabó. Holomorphic disks and three-manifold invariants: properties and applications. *Ann. of Math. (2)*, 159(3):1159–1245, 2004.
- [49] Peter Ozsváth and Zoltán Szabó. Holomorphic disks and topological invariants for closed three-manifolds. *Ann. of Math. (2)*, 159(3):1027–1158, 2004.
- [50] Peter Ozsváth and Zoltán Szabó. Heegaard Floer homology and contact structures. *Duke Math. J.*, 129(1):39–61, 2005.
- [51] Olga Plamenevskaya. Contact structures with distinct Heegaard Floer invariants. *Math. Res. Lett.*, 11(4):547–561, 2004.
- [52] William P. Thurston. Three-dimensional manifolds, Kleinian groups and hyperbolic geometry. *Bull. Amer. Math. Soc. (N.S.)*, 6(3):357–381, 1982.
- [53] William P. Thurston. *The geometry and topology of three-manifolds. Vol. IV.* American Mathematical Society, Providence, RI, [2022] ©2022. Edited and with a preface by Steven P. Kerckhoff and a chapter by J. W. Milnor.
- [54] Bülent Tosun. Tight small Seifert fibered manifolds with $e_0 = -2$. *Algebr. Geom. Topol.*, 20(1):1–27, 2020.
- [55] Hao Wu. Legendrian vertical circles in small Seifert spaces. *Commun. Contemp. Math.*, 8(2):219–246, 2006.

DEPARTMENT OF MATHEMATICS, UNIVERSITY OF CALIFORNIA, LOS ANGELES, CA

Email address: hkmin27@math.ucla.edu

DEPARTMENT OF MATHEMATICS, UNIVERSITY OF GLASGOW, GLASGOW, SCOTLAND

Email address: Isacco.Nonino@glasgow.ac.uk